JOURNAL OF MATERIALS SCIENCE 18 (1983) 2215–2240

Review
Decomposition processes in Al–Zn–Mg alloys

H. LÖFFLER
Pedagogical University, Halle, GDR
I. KOVÁCS, J. LENDVAI
Institute for General Physics, Loránd Eötvös University, Budapest, Hungary

This review surveys the present knowledge of the mechanisms of decomposition processes in Al–Zn–Mg alloys. The various experimental observations connected with the formation and properties of the different second phase particles are described and critically analysed. The effect of different heat treatments, compositions, impurities, etc on the different stages of the decomposition process is discussed in detail.

1. Introduction

During the last decade a large number of papers dealing with the decomposition processes in Al–Zn–Mg alloys appeared in the literature. The wide interest in these alloys is due to their technological importance as medium to high strength materials.

In most cases the investigations involved two or more step ageing treatments during which complicated precipitation structures are developed. The main aim is in general to improve the mechanical properties of the alloys, i.e. to find the best combination of ductility and strength, to increase fatigue endurance or to decrease their stress–corrosion sensitivity.

The aim of this paper is to review the results connected with the decomposition processes taking place in alloys in a wide range of composition after different prehistories. Since the decomposition processes depend sensitively on the composition and the details of prehistory, different authors arrive at conclusions which seem to be contradictory. However, in many cases they can be reconciled if the proper experimental conditions are taken into account.

We shall restrict ourselves only to discuss the mechanisms of the decomposition and we shall not deal with many important problems like mechanical properties or stress corrosion, etc.

In this review, unless otherwise stated, the concentrations are given in atomic per cent.

2. Decomposition processes in one-step ageing

2.1. Introduction

The ageing treatment of the Al–Zn–Mg alloys starts in most cases with a natural ageing after solution treatment and quenching. The decomposition of the supersaturated solid solution near room temperature takes place by the formation of Guinier–Preston (GP) zones. At somewhat higher ageing temperatures there is the formation of other metastable precipitate phases, while at still higher temperatures the formation of the stable (or equilibrium) phases can be observed. The structure and composition of the metastable and stable precipitates is, of course, strongly dependent on the alloy composition and on the ageing temperature. In the practical alloys GP zones, η' transition phase, η and T stable phases are forming, so we shall concentrate on the properties of these precipitates in our review.

The precipitation of the metastable and stable phases are not independent from each other. The formation of metastable precipitates has a strong influence on the nucleation of more stable phases. This fact is widely used to attain optimum properties by multiple-step ageing, the problems of which will be reviewed in detail in Section 3. However, before coming to this it is necessary to summarize the present knowledge concerning the formation and structure of the most important metastable and stable precipitates.

0022–2461/83 $03.00 + .12

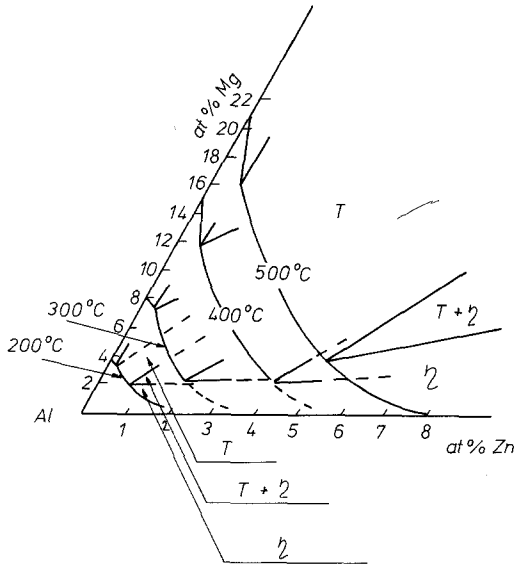

Figure 1 The aluminium corner of the Al–Mg–Zn equilibrium diagram.

2.2. Equilibrium phases

The phase diagram of the Al–Zn–Mg system was first determined by Köster *et al.* [1, 2] and it was corrected from the data of many other authors by Mondolfo [3]. The aluminium corner of the equilibrium diagram according to Mondolfo, is shown in Fig. 1. It can be seen that by disregarding the ranges of very high and very low Zn/Mg ratios two types of equilibrium precipitate phases exist: the binary $MgZn_2$ phase, usually denoted as η and the ternary $Mg_3Zn_3Al_2$ phase, usually designated by T.

The $MgZn_2$ η-phase is hexagonal with 12 atoms in the unit cell and space group $P6_3/mmc$. The lattice parameters of the $MgZn_2$ were found within the range $a = 0.516$ to 0.522 nm, $c = 0.849$ to 0.855 nm [4]. In ternary alloys up to 3% Al can be dissolved in the η-phase [5]. The equilibrium precipitates of the $MgZn_2$ phase have incoherent interphase boundaries with the aluminium matrix. The different orientation relationships between matrix and precipitate, as summarized by Degischer *et al.* [6] are listed in Table I.

The composition of the ternary T-phase varies between relatively wide limits: from 20 to 35% Mg and from 65 to 22% Zn [1, 2, 13]. The formula $(AlZn)_{49}Mg_{32}$, which is more accurate or the $Mg_3Zn_3Al_2$, which is more simple characterize its composition [14]. The T-phase is cubic; space group $Im3$ with 162 atoms in the unit cell. The lattice parameter increases from 1.429 to 1.471 nm with increasing zinc content [13, 14]. The particles of the T-phase are incoherent with the aluminium matrix and the orientation relationships

$$(100)_T \| (112)_{Al};\ (001)_T \| (1\bar{1}0)_{Al}$$

have been found [8, 15]. Ryum [16] in a more recent work reported the orientation relationships

$$(100)_T \| (1\bar{1}0)_{Al};\ (010)_T \| (111)_{Al}$$

$$(100)_T \| (110)_{Al};\ (0\bar{1}1)_T \| (001)_{Al}$$

$$(100)_T \| (110)_{Al};\ (025)_T \| (110)_{Al}.$$

As can be seen in Fig. 1, the formation range of the T-phase becomes more narrow with decreasing temperature than that of the η-phase, which coincides with the observation that in the alloys of practical interest T-phase is only precipitating at temperatures higher than 200° C [8]. In the alloys with Mg/Zn ratios between about 1:2 to 1:3 the η-phase is the only stable precipitate at lower temperatures and T at the higher ones. Therefore some authors consider, in this case, η as an intermediate phase [8, 17, 18], which could transform to the T-phase. Mondolfo has shown,

TABLE I Orientation relations (except for η_{10}, η_{11} the notation of Gjønnes and Simensen [7] is used)

N	Orientation relations			Shape	SG [8]	Th [9]	A [10]	Others
η_1	$(00.1)\|\|(110)$	$(10.0)\|\|(001)_\alpha$		Plates	*a*	6	5	–
η_4	$(00.1)\|\|(110)$	$(\bar{1}2.0)\|\|(1\bar{1}\bar{1})_\alpha$		Rods	–	1	4	–
η_5	–	$(\bar{1}2.0)\|\|(1\bar{1}\bar{1})_\alpha$	$(30.2)\|\|(110)_\alpha$	Rods	–	2	–	–
η_6	–	$(\bar{1}2.0)\|\|(1\bar{1}\bar{1})_\alpha$	$(20.1)\|\|(1\bar{1}2)_\alpha$	Rods	–	3	–	–
η_7	–	$(\bar{1}2.0)\|\|(1\bar{1}\bar{1})_\alpha$	$(10.4)\|\|(110)_\alpha$	Rods	–	4	–	–
η_9	$(00.1)\|\|(110)$	$(\bar{1}2.0)\|\|(001)_\alpha$		Laths	–	–	3	[11]
η_{11}	$(00.1)\|\|(110)$	$(10.0)\|\|(1\bar{1}\bar{1})_\alpha$		–	–	–	–	[6]
η_2	$(00.1)\|\|(1\bar{1}\bar{1})$	$(10.0)\|\|(110)_\alpha$		Plates	*b*	5	1	–
η_3	$(00.1)\|\|(1\bar{1}\bar{1})$	$(11.0)\|\|(110)_\alpha$		Plates	*c*	–	2	[12]
η_{10}	$(001)\|\|(1\bar{1}\bar{1})$	$(11.0)\|\|(1\bar{3}4)_\alpha$		–	–	–	6	–
η_8	$(00.1)\|\|(31\bar{1})$	$(\bar{1}2.0)\|\|(1\bar{1}2)_\alpha$		Rods	–	–	–	–

however, that in an Al–6%Zn–2%Mg alloy the $MgZn_2$ η-phase remained stable even after an 8000 h annealing at 200° C [3]. The size of the critical nucleus of the T-phase is large and as a consequence of this a coarse precipitate structure with large particles is forming which does not give rise to considerable precipitation hardening. So the appearance of the T-phase coincides with the overageing of the alloy.

2.3. Metastable precipitate phases

According to most authors, in the age-hardenable Al–Zn–Mg alloys, the decomposition of the supersaturated solid solution (SSSS) takes place in general by the following sequence [8, 18–24]:

SSSS → GP zones → intermediate

→ final precipitates.

The sequence of steps in the decomposition process, however, strongly depends on the composition of the alloy, on the quenching conditions, on the ageing temperature, etc [6–9, 11, 18–64]. Most of these problems will be reviewed in Section 3. Here we try to summarize the most important results concerning the structure and formation of GP zones and η' precipiates.

2.3.1. GP zones

2.3.1.1. Some general properties of GP zones in Al–Zn–Mg alloys. X-ray techniques provide the most direct information on the structure of GP zones. The first X-ray diffraction investigations on GP zones in Al–Zn–Mg alloys were carried out by Graf [65, 66]. According to his results GP zones consist of layers parallel to the (100) matrix planes enriched and impoverished in zinc alternately, which is shown by the appearance of (100) super-reflections.

Schmalzried and Gerold [8] studied the decomposition process in an Al–2.6%Zn–3.9%Mg alloy applying the oscillating single-crystal method and small-angle X-ray scattering (SAXS). They observed that weak, diffuse (100) super-reflections appear already in the course of room temperature ageing. They interpreted their results by assuming that during GP zone formation the (001) planes become enriched in zinc or in magnesium alternately and hence, as a consequence of the opposite size effect of the two alloying elements [4], the lattice spacing of the matrix remains unchanged in this direction. The intensity distribution did not become narrower and stronger even after 4 months of natural ageing. At 100° C, however, weak reflections of the hexagonal η'-phase could be detected after 8 h, besides the (100) super-reflections, characteristic of the GP zones.

Gerold and co-workers [67–69] have shown that in binary alloys the composition of the precipitates or GP zones can be determined by the measurement of the integrated intensity of SAXS on a series of alloys of different compositions. If the atomic volumes in the second phase particles and in the remaining solid solution are the same then the integrated intensity (Q) of SAXS can be described by the following equation:

$$Q = (X_1 - X)(X - X_2)\frac{(\Delta b)^2}{V_a} \qquad (1)$$

where X_1 and X_2 denotes the atomic fraction of the alloying element in the particles and in the remaining solid solution, respectively, X is the average atomic fraction of the alloying element, Δb is the difference in the scattering power of both elements and V_a is the atomic volume.

The method of Gerold and co-workers has been generalized for the determination of the zinc concentration of GP zones in Al–Zn–Mg alloys by Dünkeloh *et al.* [55, 70]. The method makes use of the fact that the scattering amplitude of magnesium and aluminium for X-rays are very close to each other. The difference in atomic volumes in the particles and in the matrix could be taken into account in Equation 1 [69]. At present, however, we are missing reliable data on atomic volumes in metastable precipitate phases of the Al–Zn–Mg system [71, 72]. Results of Dünkeloh *et al.* for Al–Zn–Mg alloys with Zn/Mg=2 give 40% Zn within the GP zones in metastable equilibrium at room temperature with a solid solution containing 0.8 Zn [55].

An independent method (e.g. neutron small-angle scattering) is needed to determine the position of the tie-lines in the ternary metastable equilibrium diagram and to obtain the magnesium concentration of the GP zones [71, 72]. Because of difficulties in the evaluation of the neutron SAS (small-angle scattering) measurements, however, the magnesium concentration in the GP zones could be determined by Gerold *et al.* [72] only with a rather high uncertainty.

Groma *et al.* [73] have shown by applying only SAXS measurements that for the case of alloys with $0.5 \leqslant Zn/Mg \leqslant 2$ the zinc content of the GP zones in metastable equilibrium at room tempera-

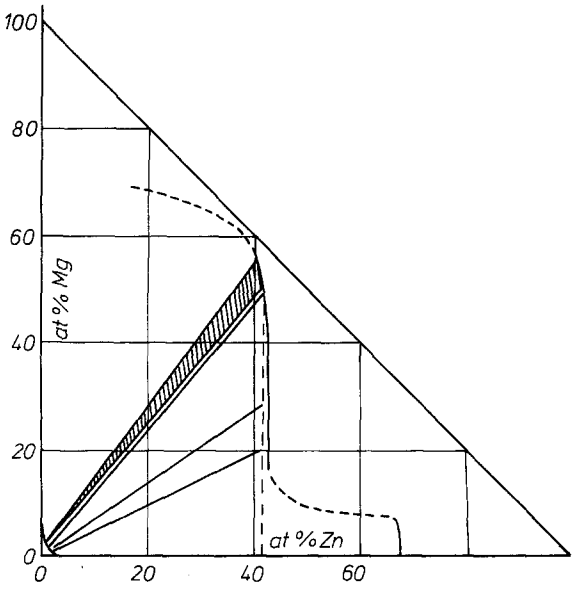

Figure 2 The metastable miscibility gap of Al–Zn–Mg alloys at room temperature.

ture does not deviate strongly from 40%, while the magnesium concentration of the zones varies from 20 to about 60% as a function of the Zn/Mg ratio. Unpublished work of Ungár shows that if the Zn/Mg > 2 the zinc content of the GP zones at room temperature may exceed 40% and with extremely high Zn/Mg ratios it tends to about 70% which is the value obtained in binary Al–Zn alloys [74]. The phase diagram of Al–Zn–Mg alloys with the metastable miscibility gap is shown in Fig. 2. According to Gould and Starke [44], Suzuki *et al.* [75] and Tomita *et al.* [56] in alloys with low magnesium content ternary Al–Zn–Mg zones coexist with zones containing only zinc and aluminium. The coexistence of this two types of GP zones was confirmed by calorimetric investigations of Honyek *et al.* [76] in alloys with Zn/Mg > 9.

2.3.1.2. The temperature dependence of GP zone formation. After quenching Al–Zn–Mg alloy samples to different ageing temperatures an upper limit of temperature can be observed above which no GP zone formation can be detected. In the following this temperature is denoted by T_h.

The most direct method is to determine T_h by TEM investigations. As a function of the ageing temperature an abrupt change in the density of precipitates was observed on alloys with compositions Al–4.5%Zn–2.5%Mg at $T_h = 175 \pm 5°$ C [77], Al–3%Zn–3%Mg at $T_h = 155°$ C [32] and Al–2.2%Zn–1.2%Mg at $T_h = 120 \pm 5°$ C [78]. Similar observations can be made by other methods, such as SAXS, electrical resistivity and mechanical properties measurements. By SAXS investigations Kawano *et al.* [48] have found $T_h = 115°$ C for the alloy Al–2.8%Zn–1.4%Mg. The results of Zahra *et al.* [64] obtained by calorimetric measurements show $T_h = 115°$ C for the alloy Al–2.12%Zn–1.26%Mg. In a recent investigation on an Al–2%Zn–1.5%Mg alloy Inoue *et al.* [79] obtained $T_h = 125°$ C.

According to many investigations the basic properties of the alloy system are not changed considerably by varying the magnesium content within relatively wide range of concentrations [33, 73]. On the basis of this fact a metastable phase diagram can be constructed taking into account only the zinc concentrations [80]. This diagram is shown in Fig. 3 in which the upper limit of the zone formation is given by the curve T_h.

Polmear [30, 31] and Lorimer and Nicholson [32] identified T_h in Al–Zn–Mg alloys as the metastable phase boundary, in our opinion it is more clearly defined by the above manner, i.e. as the highest temperature at which GP zones can be formed after a direct quench to the ageing temperature, because the dissolution line of GP zones is necessarily shifted to somewhat higher temperatures (Fig. 3).

There are many observations according to which GP zones formed at higher ageing temperatures are different of those formed at or near room temperature. Investigations by Graf [65, 66, 81], Mondolfo *et al.* [20], Schmalzried and Gerold [8] and Gerold and Haberkorn [82] indicated that at 100° C GP zones form on (111) matrix planes unlike the room temperature GP zones which form on (100) planes. The GP zones formed parallel to the (111) matrix planes show internal order, and after prolonged ageing their structure becomes similar to that of the η' precipitates. According to investigations made on more concentrated alloys [19, 41] there is no evidence for the formation of two different types of GP zones. Kelly and Nicholson [19] consider the internally ordered particles observed by Graf and others as η' precipitates.

In an Al–2%Zn–2%Mg alloy after 5 min ageing at 100° C or 2 min ageing at 150° C spherical particles of 2.5 nm diameter have been observed by high resolution bright-field electron microscopy

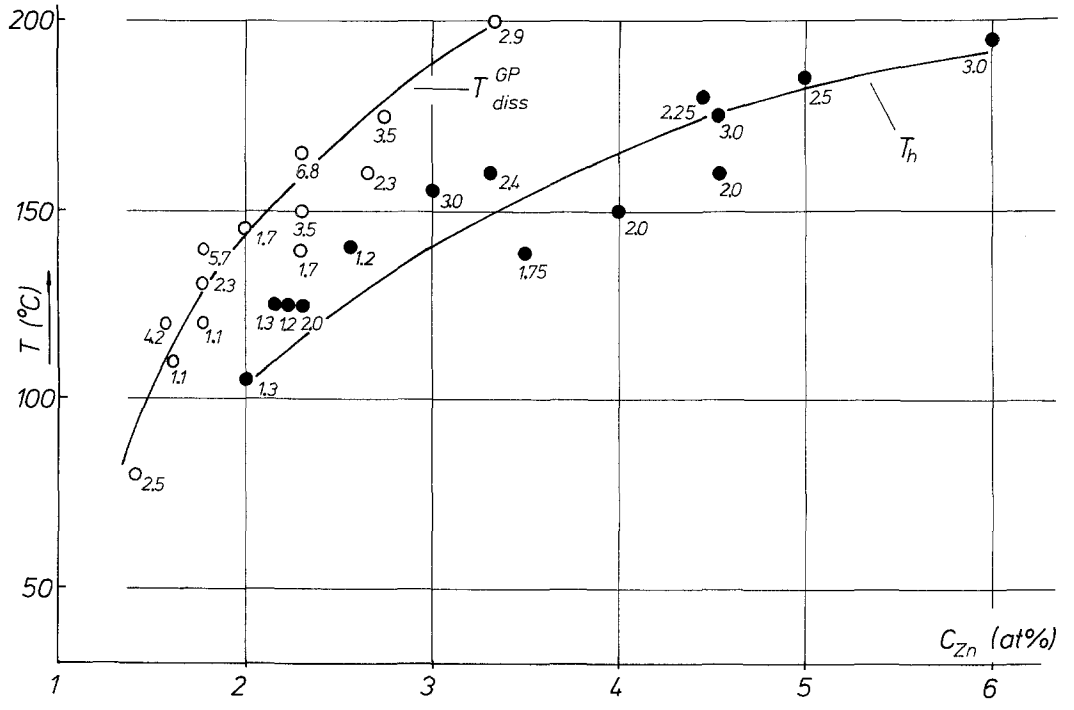

Figure 3 The upper temperature limit of GP zone formation, T_h, and the dissolution line of GP zones, T^{GP}_{diss} as a function of zinc concentration. (Numbers at the points indicate magnesium concentration.)

[58]. The particles are coherent with the (111) planes of the matrix. Later on they transformed into the plate-like η' particles. Similar results were obtained by Brofman and Judd [61]. SAXS investigations on an Al–2%Zn–1.3%Mg alloy revealed one type of GP zones up to 60° C, while between 60 and 100° C fully coherent particles with two different average diameters have been observed [83]. Calorimetric investigations on the same alloy confirmed the coexistence of two types of particles in the temperature range between 60 and 100° C [64, 84]. Results of Ungar [83] show that at about 100° C the particles with larger average size coexist with the η' precipitates and after reaching a definite size they can transform into the η' particles. Taking into account these results it might be of more consequence to consider these fully coherent precursors of the η' phase as GP zones and to call them GPII zones to distinguish them from the ones formed near room temperature [83].

To distinguish more definitely between these problems further work is needed, particularly by studying the structure changes in a wide range of temperatures and compositions.

2.3.1.3. The effect of quenching conditions on GP zone formation. The decomposition process at about room temperature in Al–Zn–Mg alloys sufficiently rich in magnesium was often found to be independent of the quench conditions applied, which means the temperature of the solution heat treatment, T_q, and the quenching rate, v_q (see e.g. [60, 85–90]). As reported by Ryum [16, 57] even an interruption of the quench for 1 min at 200° C (step-quench) did not remarkably alter the change of the Vickers microhardness (HV) of the samples at room temperature (Al–2.8%Zn–1.24%Mg alloy).

There are indications, however, that these statements hold only for the later stages of ageing, the early part of the decomposition process depends on the quench conditions [64, 89, 90]. In this section we summarize some characteristic results obtained in this field.

In Fig. 4 the results of resistivity measurements performed on an Al–3%Zn–0.76%Mg alloy are presented [89]. The annealing temperature, T_q, was varied between 360 and 480° C. The samples were quenched into water of temperature T_a, and the resistivity was measured *in situ* as a function of

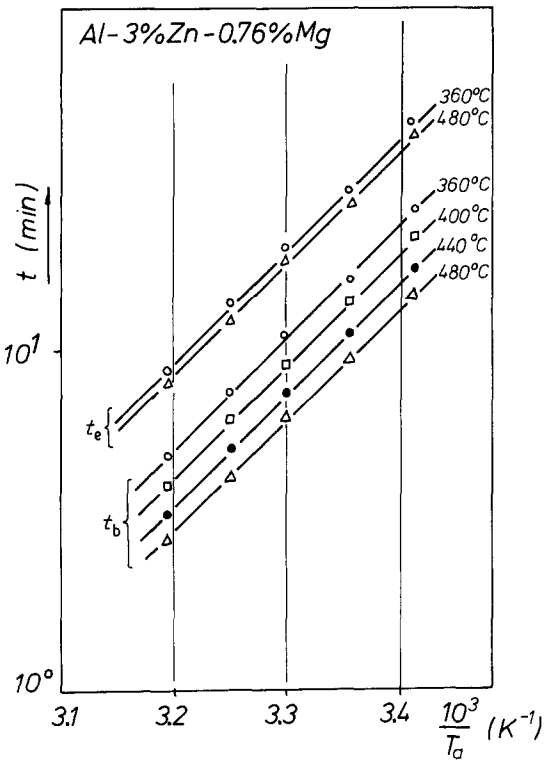

Figure 4 Ageing start and end times, t_b and t_e, respectively, of the linear part of the R–ln t curves against reciprocal temperature. (Samples were directly quenched from temperatures indicated, to T_a.)

time. In Fig. 4 the start and end times t_b, and t_e, respectively, of the linear part of the R–ln t curves are plotted as functions of the reciprocal temperature. It can be seen that t_b depends sensitively on T_q, but t_e is practically independent of it. The quench-sensitivity at the start of the decomposition was also confirmed by isothermal hardness measurements [90].

The effect of quenched-in excess free vacancies on the formation of GP zones at or near room temperature is not quite clear. Few authors have investigated this problem by systematic alteration of the vacancy concentration [85, 91]. According to many observations the quenched-in free vacancies have no significant effect on the formation of GP zones at or near room temperature. So it is widely accepted that, in contrast to the effect in binary Al–Zn alloys, the number of quenched-in free vacancies has practically no influence on the GP zone formation in ternary Al–Zn–Mg alloys [42, 87, 88, 92]. This difference is most probably due to the strong binding energy between vacancies and magnesium atoms.

Apart from a relatively short initial period the GP zone formation was observed to become significantly slower by adding magnesium to binary Al–Zn alloys [87, 93], from which it was concluded that the kinetics of zone formation is controlled by the motion of magnesium atoms. The probable reason for this is that most of the quenched-in vacancies are bound to magnesium atoms [39, 46, 85, 92, 94]. This is further supported by the fact that the activation energies observed in the early part of the zone formation process are all near to the migration energy of magnesium atoms in aluminium [8, 53, 95]. On the other hand there are many observations according to which the zone formation starts with the formation of zinc or zinc–vacancy clusters [39, 92–97]. There are indications [98] that, probably as a consequence of the opposite size effect of the zinc and magnesium atoms in aluminium, a strong attractive interaction between the zinc and magnesium atoms is effective even at the solution-treatment temperature. This is supported by the observations of Juhász *et al.* [99] according to which solute clusters are forming within a few minutes after quenching in which the average Zn/Mg ratio is 4:1. The further process is controlled by the migration of magnesium atoms or Zn–Mg–vacancy clusters [89], the activation energy of which is close to that of the magnesium atoms.

2.3.1.4. The kinetics of GP zone formation. The kinetics of GP zone formation in Al–Zn–Mg alloys has been studied by many authors applying different methods, mainly electrical resistivity, hardness and SAXS measurements [53, 89, 100, 101]. The results, however, are rather contradictory concerning both the time dependence and the activation energy of the process. A possible explanation for this might be the different compositions of the alloys investigated.

Electrical resistivity of ternary Al–Zn–Mg alloys was found to increase continuously during room temperature ageing after quenching and in contrast to binary Al–Zn alloys a resistivity maximum could not be observed except in alloys with a very low Mg/Zn ratio [46, 85, 93] or with a high zinc content (about 6%) (e.g. [43, 44]). The hardness as a function of ageing time at room temperature starts with an incubation period then it increases linearly with the logarithm of time, thereafter a plateau appears [31, 42, 102, 103]. After this another strong increase in hardness can be

observed in special conditions [6, 18, 54]. Dünkeloh *et al.* [55] observed by SAXS measurements that the radius, r of the GP zones increased linearly with the logarithm of ageing time. The slope of the r–ln t curve was independent of the concentration in the case of the Al–$MgZn_2$ type alloys investigated. In many cases an $r \sim t^m$ law is observed. According to the TEM investigations of Lyman and Vander Sande [58] the mean size of GP zones increases linearly with $t^{1/9}$.

According to experimental results at temperatures between room temperature and 60° C two stages in the formation of GP zones can be well distinguished [101]. In the very early stage both the integrated intensity of SAXS and the electrical resistivity can be described by a Cottrell–Bilby type kinetics. The duration of this stage is strongly influenced by the temperature of ageing and by the composition of the alloy. It changes between about 10 and 100 min. Plotting the logarithm of the time corresponding to the end of this stage as a function of the reciprocal of the ageing temperature, an activation energy of 0.62 eV was obtained independently from the quenching conditions and from the alloy composition. Panseri and Federichi [85] have shown that the addition of as little as 0.1% Mg to the binary Al–Zn alloys is enough to raise the activation energy of the zone formation process from the value characteristic of the zinc migration (0.4 eV) to 0.6 eV. A similar conclusion was reached, for example, by Ceresara and Fiorini [53] on Al–Zn–Mg alloys with 2 and 3% Mg. The value of about 0.6 eV is generally considered as the migration energy of magnesium. Taking this into account and the fact that the SAXS is sensitive only to the clustering of zinc atoms one can conclude that both the zinc and magnesium atoms take part in this stage of the zone formation but the rate of the process is controlled by the motion of magnesium atoms.

After an intermediate process a second stage is observed which can be described by an Avrami kinetics [101].

A dependence of the reaction rate of the initial process on the zinc concentration was also observed which indicates that during quenching or immediately after it small Zn-rich clusters are formed which become the nuclei of the GP zones. The formation of these clusters must have been finished within 1 min after quenching as after this time both zinc and magnesium atoms are migrating in the matrix. The process proceeds further by the formation of nuclei of zones on these clusters. The rate of this process is controlled by the migration of magnesium atoms and by vacancies bound to solute atoms or to solute atom clusters. In the next stage the zones are growing and the process is slowed down probably by the appearance of coherency strains and by the decrease in supersaturation.

2.3.2. The η' phase

Graf [65] was the first to observe that the diffuse X-ray diffraction pattern characteristic of GP zones changes at about 80 to 100° C, the (100) reflection disappears gradually while the (200) reflection becomes more and more pronounced. The structure of the precipitates becomes similar to that of the η-phase but it is not the same. Graf determined the structure of the η' transition phase [66], which is hexagonal with $a = 0.496$ nm, $c = 6\, d_{[111]\,Al} = 1.403$ nm. Mondolfo *et al.* [20] determined the lattice parameters of the η' precipitates as $a = 0.496$ nm, $c = 0.868$ nm. Results of Thomas and Nutting [21] confirmed the c-value of Mondolfo *et al.*, whereas Auld and Cousland [104, 105] confirmed the value obtained by Graf. Gjønnes and Simensen [7] as well as Auld and Cousland [104, 105] interpreted η' in terms of a monoclinic structure with $a = b = 0.497$ nm, $c = 0.554$ nm and $\gamma = 120°$. In general for the composition of the platelike η' particles $MgZn_2$ is accepted, but according to Auld and Cousland it is better described by the formula $Mg_4Zn_{11}Al$ [105]. They found the orientation relationships

$$(0001)_{\eta'} \| (1\bar{1}1)_{Al};\ (10\bar{1}0)_{\eta'} \| (110)_{Al}.$$

More recently Chou [106] has observed another orientation relationship for the case of spherical, partially coherent η' particles having the same lattice parameters:

$$(00\bar{1}0)_{\eta'} \| (100)_{al};\ (0001)_{\eta'} \| (01\bar{1})_{Al}.$$

According to Mondolfo *et al.* [20] the formation of the η' transition phase starts by the segregation of alloying elements on stacking faults. As a consequence of the differences in atomic sizes coherency is gradually lost and the ordered structure of the η-phase develops. This would mean that there is a continuous transition from the supersaturated solid solution to the precipitation of the η-phase.

There are other investigators assuming that the nucleation of the η' particles takes place at stacking faults [11, 21] but there is no direct observation for this assumption. Embury and Nicholson [11] studied the nucleation of the η' transition phase in an alloy containing 2.46% Zn and 3.2% Mg. They investigated the precipitate free zones (PFZ) along grain boundaries after direct quenching to the ageing temperature and concluded that in the case for a given alloy composition the vacancy concentration, C_v, has to reach a certain critical value, C_{cr}, to make a quasi-homogeneous nucleation (a homogeneously distributed dense system) of the η' particles possible. According to Embury and Nicholson [11] the nuclei for the homogeneous η' precipitation are vacancy–solute clusters (cf. Section 3.3).

On the basis of microhardness measurements and TEM investigations carried out on an Al–2.4%Zn–1.2%Mg alloy Ryum [57] assumes that nuclei of η' particles consisting of very small vacancy–solute clusters are formed during the quenching or immediately after it at room temperature. These nuclei form within 5 sec after quenching and remain stable at low temperature ageing. They do not take part in GP zone formation, but they can serve as nuclei for η' formation in a subsequent ageing at about 150° C even after a long period of pre-ageing.

Radomsky *et al.* [107] confirm the importance of vacancy–solute clusters in the nucleation of the η' precipitates especially in case of relatively low concentration alloys ($C_{Zn} < 2.5\%$; C_{Mg} about 1 to 2%), however, in contrary to Ryum [57] they observed changes in the number of the nuclei even during room temperature ageing. In the case of more concentrated alloys they find the GP zone → η' transition to be the dominant mechanism in η' formation.

3. Decomposition processes in multiple-step ageing

3.1. Introduction

In the middle of the 1960s it had become increasingly apparent that the simple picture of precipitate nucleation, namely, that the dispersion of precipitates is controlled by the solute supersaturation, is principally incorrect in three respects [11]: the degree of dispersion is

(a) frequently very different in alloys of similar solute supersaturation,

(b) highly inhomogeneous both from one grain to another and within individual grains, and

(c) sensitive in many alloys to the quenching rate, the time interval at room temperature before final ageing, the rate of heating to the ageing temperature, T_a, and the presence of trace elements, none of which appreciably affect the solute supersaturation.

In the last two decades a large number of investigations were performed to obtain more insight into the nature of the decomposition processes of the Al–Zn–Mg alloys. In most cases the investigations involved two or more step ageing treatments. The results of such experiments have important practical applications. The main aim is, in general, to improve the mechanical properties of the alloys, for instance to find the best combination of ductility and strength [108] or to improve the fatigue endurance [109], and to decrease their stress–corrosion sensitivity. The multi-step ageing treatment can also help to avoid the diminution of the strength in polygonized materials [34].

The aim of this section is to summarize the main results obtained by the various authors in this field and to look for common features of the phenomena observed, which are sufficiently independent of alloy composition, technical impurities, variations of heat treatments and the methods of investigations applied. We shall try to check the validity of the different models proposed to explain the processes taking place during the various steps of multiple-step ageing treatments, and to find proper ordering principles characteristic to the alloy system.

3.2. GP zones as potential nucleation sites for more stable phases

The formation of nuclei of partially and fully incoherent precipitates needs more surface energy than the creation of coherent GP zones. It can be expected, therefore, that in one-step ageing the nucleation of η' or equilibrium phases can take place first of all heterogeneously at favourable places like grain boundaries, dislocation loops and dislocations. GP zones nucleated and grown during a pre-ageing treatment can also be expected to act as nucleation sites for the heterogeneous formation of, for example, the η'-phase at suitable ageing temperatures.

The fact that GP zones can act as potential nucleation sites of more stable precipitate particles

provides the basis of double ageing treatments applied to Al–Zn–Mg alloys. The respective theories of such processes have been outlined by Lorimer and Nicholson [32] and Pashley and co-workers [110, 111]. Apart from small differences, both theories are basically similar in their conclusions. One of the important predictions of these double-ageing theories is that the number of precipitates formed during the second step ageing is a function of the zone size distribution. The larger the average zone size and density, the greater the number of precipitates.

The positive influence of the presence of GP zones on the η'-phase formation results from the fact that the number of zones as nucleation sites can be much larger than the number of η' nuclei which would be formed in one-step ageing [112].

On the basis of this picture the role of quenched-in vacancies is considered merely to increase the rate of GP zone formation by accelerating the diffusion during pre-ageing. They probably have no direct influence on the formation of η'-phase as assumed by many authors [11, 16, 39, 57, 113–118]. We will return to the influence of vacancies on the nucleation of η'-phase precipitates in Section 3.3.

3.2.1. Indications of the direct sequence GP zones → η'-phase at $T_a > T_h$ (partial dissolution of GP zones, reversion)

The strength of the alloy and the volume fraction of the GP zones in low concentration Al–Zn–Mg alloys age-hardened, for example, at room temperature rapidly decreases to the values corresponding to the as-quenched state when the alloy is heated up to a sufficiently high temperature for a short time. This phenomenon was first detected by few authors in the 1920s [119–122] and called "the reversion". Gerold [123] first considered the reversion as re-dissolution of GP zones. In specimens showing such a behaviour the GP zones formed during pre-ageing at temperature T_{pre} cannot act directly as nucleation sites for the η'-phase as proposed by Lorimer and Nicholson [32], because the GP zones are completely dissolved before the nucleation and growth of the intermediate phase starts. These cases will be considered in Section 3.2.2. Here we deal with such cases, when the dissolution of zones and the formation of η'-phase "overlap", which means, that the physical quantities measured after reversion do not reach the as-quenched level. We call this phenomenon "partial reversion". Whether a partial reversion is an indication for the direct sequence of GP zones η'-phase transformation (some overcritical) GP zones are directly transformed into η' particles) or the dissolution of the individual zones is complete (i.e. true reversion takes place), but the nucleation and growth of η' precipitates starts before the total dissolution of the zones, is an important problem. We shall discuss this problem in detail. Now we only summarize experimental indications for partial reversion in Table II.

From Table II it can be concluded that partial reversion appears in Al–Zn–Mg alloys of great variations of alloy composition, pre-ageing temperature and time, and ageing temperature or heating rate applied. Unfortunately most of the reversion experiments do not start from states characterized by the density, composition and size distribution of the precipitate particles, but in most cases the starting conditions are given by the ageing time and temperature, maximum resistivity or hardness and so on. This fact makes the interpretation of the results more difficult.

Many authors explain the partial reversion presuming overcritically sized GP zones which can directly transform into nuclei of the η'-phase [e.g. 11, 20, 21, 25, 28, 34]. Other authors assume that during pre-ageing two types of clusters, namely GP zones and vacancy-rich clusters of solute atoms [16, 57, 139] or GP zones and nuclei of the η'-phase [112, 140] are formed simultaneously. These nuclei of the η'-phase and the vacancy-rich clusters are both able to grow into η' particles at elevated temperatures. It is also possible that during pre-ageing two different types of GP zones are formed (cf. Section 2.3.1.2) from which the less stable ones (GPI zones) dissolve at the beginning of the second-step ageing, while the more stable ones (GPII zones) transform directly into η' particles [83, 84, 141, 142].

We shall discuss this problem in Section 3.5.

3.2.2. Complete reversion

Many authors (see Table III) reported that GP zones formed at T_{pre} completely dissolve at $T \geqslant T_R$ before the formation of η'-phase particles. T_R is called the temperature of reversion. This phenomenon is called complete reversion. In spite of the complete dissolution of the zones, such treatments often result in finely distributed η' particles, while in specimens directly quenched to

TABLE II Investigations showing partial reversion in Al–Zn–Mg alloys pre-aged at $T_{pre} < T_h$ during subsequent ageing at $T_a > T_h$ or during upheating from T_{pre} to T_a with a heating rate, v_h

c_{Zn}(%)	c_{Mg}(%)	t_{pre}, T_{pre}	Methods	T_a or v_h	Quenching treatment	Reference
3.0	1.0	$1.4.10^6$ min	SAXS	$0-10^4$ sec	1 h 480° C	[124]
	1.5	RT		110–130° C	H_2O(RT)	
	2.9					
6.0	0.5	1 week	SAXS,	100° C	5 h 480° C	[125]
	1.3	50° C	HV,	130° C	H_2O(RT)	
	2.2		R	150° C		
	3.2					
2.4	0.9	30 or	HV	80–180	30 min 450° C	
	1.6	80 days		$T = 20$	alcohol (0° C)	
	2.5	RT				
5.71	0.079	1 week	SAXS,	165° C, 135° C,	1 h 460° C	[44]
5.76	0.29	50° C	TEM	135° C	H_2O(0° C)	
2.66	2.11	6 days	mechanical	100–200° C	3 h 440° C	[126]
		40° C	properties,		H_2O(0° C	
			TEM		max 1 min)	
4.5	0.2	1 h	SAXS	$v_h = 0.5$ K min^{-1}	30 min 450° C	[127]
	1.0	RT	TEM,		H_2O(RT)	
	2.5		PAS			
4.5	1.0	1 to 60 days	dilatometry	$v_h = 5$ K min^{-1}	30 min 450° C	[128]
			150° C		H_2O(RT)	
4.5	2.0	interrupted,	TEM		30 min 480° C	[129]
	3.0		SAXS,		H_2O(RT)	
		continuous	DTA,	$v_h = 20$ K min^{-1}		
		heating	DSC, R			
4.5	2.0	60 days	SAXS,	$v_h = 80$ K min^{-1}	30 min 480° C	[130]
	3.0	RT	TEM, DTA,		H_2O(RT)	
			DSC, R			
2.46	1.24	5, 20 sec	TEM, HV	150° C	400° C	[16, 57]
		1800 sec			H_2O(RT)	
		at RT				
2.45	2.24	1 min 21° C	TEM, HV	175° C	1 h 475° C	[16, 57]
		1 min 200° C			H_2O(21° C)	
					1 h 475° C	
					Oil (200° C)	
2.6	2.8	Maximum of HV,	HV			[131]
		9 h 175° C				
3.1	2.8	Maximum of HV,	DSC	$v_h = 10$ K min^{-1}	2 h 480° C	
			TEM,			
		21 h 163° C	mechanical		H_2O(RT)	
			properties			
2.6	2.5	4 h 120° C				
		4 h 168° C				
		24 h 120° C				
		overaged state				
2.12	1.14	24 h RT;	Calorimetry			[64]
		5 h, 24 h, 96 h				
		40° C	TEM		400, 450,	
		24 h/22 ro 40° C			500° C	
		24 h 120° C			H_2O(0° C)	
2.0	1.4	7 h–60 days	SAXS, TEM	30 min	30 min 480° C	[107]
4.5	2.5			180° C	H_2O(RT)	
		RT	mechanical			
			properties			
2.04	1.37	7 h–60 days	SAXS, R,	2 h, 4 h	30 min 480° C	[132]
				160° C	H_2O(20)	
		RT	mechanical			
			properties			

TABLE II (*continued*)

c_{Zn}(%)	c_{Mg}(%)	t_{pre}, T_{pre}	Methods	T_a or v_h treatment	Quenching treatment	Reference
4.5	1.0	1 h–60 days RT	SAXS, TEM	0–1000 min 150° C	1 h 490° C H_2O(RT)	[133]
4.5	2.0	1 h 100° C	SAXS, TEM HV	140, 160 180° C	1 h 450° C T_a 1 h 450° C 1 h 100° C T_a	[133]
4.5	2.5	1 min RT	SAXS, TEM HV, R	120–200° C	1 h 490° C H_2O(RT, 1 min) T_a 1 h 490° C Oil (T_a); T_a	[133]
2.4	1.1	0–90 days RT HB	TEM, SAXS	120, 140° C 160, 180° C aircooling	1 h 490° C	[134]
4.5	0.05 0.1 0.2 0.5 1.0 1.5 2.0 2.5 3.0	5 min, 10 days, 7 days 180 days	DSC, TEM	v_h = 80 K min^{-1}	30 min 480° C H_2O(RT)	[135]
2.52	2.87	100, 60°	HV, R,	130, 180° C	30 min 470° C	[136]
2.52	1.64	50, 70, 100° C	TEM	120, 150° C		
2.3	1.2	70° C, till HV = 1.05 GPa		180° C	2 h 500° C H_2O(0° C)	[18]
2.6	3.2	100° C, 1 h	TEM	180° C	1 h 500° C H_2O(RT)	[32]
2.4	2.9	95° C, 100 h	SAXS, R	155° C	2 h 460° C H_2O(0° C)	[137]
2.0	1.4	60 days RT + 2 h 100° C	SAXS, R mechanical properties	160° C	30 min 480° C H_2O(RT)	[138]

RT Room temperature.
DSC Differential scanning calorimetry.
DTA Differential thermoanalysis.
HB Macrohardness.
HV Microhardness.
R Resistivity, electrical.
SAXS Small-angle X-ray scattering.
TEM Transmission electron microscopy.

the same ageing temperature only coarse heterogeneously distributed η'-phase particles are formed. This different behaviour clearly proves the influence of GP zones on η'-phase formation which means that the dissolving GP zones must leave behind traces of their former existence. It is very difficult to obtain reliable information about the microstructure of these traces. Due to this fact no unique picture of the nature of these traces can be found in the literature. According to Groma and Kovács-Cseténvi [143] as a consequence of true reversion no large GP zones exist to act as nuclei for the precipitation of η'-phase and so the Lorimer–Nicholson model cannot apply, but the transformation occurs as follows: GP zones → solid solution (undersaturated with

TABLE III Complete reversion observations in Al–Zn–Mg alloys

c_{Zn}(at %)	c_{Mg}(at %)	t_{pre}, T_{pre}	Methods	t_a, T_a	Quenching treatment	Reference
1.34	2.49	60 days RT	mechanical properties R, SAXS	10 sec–2 h 120–200° C	1 h 480° C H_2O(RT)	[144]
2.68	4.0	120 days RT, 14 days 50° C	X-ray	15 sec 200° C	480° C H_2O(20° C)	[8]
2.04	1.37	Up to 180 days, t–1 min, 10 min 120 min at 80–200° C	R. SAXS, TEM, mechanical, properties	2 h 160° C 2 h or 4 h 160° C	1 h 480° C H_2O(RT)	[138]
2.08	1.26	12 h, 24 h 60. 80, 100° C	mechanical properties	0–4 h 140, 160° C	30 min 480° C H_2O(RT)	[141]
2.1	1.05	RT–100° C		170–220° C $v_h = 1$ K min^{-1}	2 h 500° C H_2O(0° C)	[18]
3.0	1–3	3 years	SAXS	120° C	1 h 480° C	[124]
2.5	2.8	RT			H_2O(RT)	
2.5	1–3	60 days RT	DSC	$v_h = 80$ K min^{-1}	1 h 480° C H_2O(RT)	[80]
1.4	2.7	1 year RT	R	155° C	1 h 470° C H_2O(0° C)	[143]

For explanations of R, DSC, etc. see footnotes to Table II.

respect to GP zones and supersaturated with respect to η'-phase) → η'-phase. It is possible that the η'-phase nucleates heterogeneously on the small clusters produced in the final stage of dissolution of the zones; this might explain the effectiveness of two-step ageing. From combined investigations of the volume fraction of zones, f, the electrical resistivity, R, and the yield stress, Y, during reversion of a relatively low concentration alloy it was concluded [138, 144, 145] that the zones dissolve completely, but the reverted state is not due to a homogeneous solid solution. It is plausible to make the assumption that concentration fluctuations rich in zinc and magnesium will be left behind by the zones. The alloy can be considered in a quasi solid solution state. This means that in the reverted state of the alloy both the SAXS and R behave as in the solid solution state and only the mechanical properties (Y did not drop abruptly like f and R to the solid solution state, but smoothly) indicate that this kind of solid solution is not homogeneous.

According to Gerstenberg [124] the dissolution of GP zones starts with the decrease of their zinc content, the rate of which decreases with the increase of the size of zones. This means that small dissolving GP zones can cause a high local supersaturation of the matrix, which is diminished by the formation of η'-phase. The local enrichment of solute atoms in the vicinity of the dissolving zones can play therefore an important role in the formation of η'-phase.

In Table III results of investigations indicating total reversion during two-step ageing as well as during continuous heating are summarized. From Tables II and III it can be concluded that specimens quenched to room temperature and aged for a certain time become totally reverted if the zinc content does not exceed about 2.5%. However, applying higher pre-ageing temperatures (between 40 and 100° C) [18, 64, 109, 138] or air-cooling to room temperature followed by 7 day storage at room temperature [146] specimens having zinc contents less than 2.5% (down to about 2.1%) become also only partially reverted. This means that the stability of zones against reversion heat treatments depends on the pre-ageing treatment (quenching or cooling to room temperature, pre-ageing temperature) or in other terms, on the size distribution and probably the composition of GP zones. The stability of GP zones during reversion will be discussed further in Section 3.5.

3.3. Vacancy-rich clusters as nucleation sites for the η'-phase

Several authors interpreted the differences of the precipitate structures obtained after direct quench, DQ, and indirect quench, IQ, to T_a assuming that in the latter case agglomerates of vacancies and

alloying atoms (called vacancy-rich clusters, VRC) are formed in the vicinity of room temperature either during the quench and/or during short ageing times (order of 10 sec), which can act as nucleation sites for the η'-phase (or even η-phase) during ageing at T_a [16, 57, 112, 118, 140]. It is generally accepted that pre-ageing times of 30 sec or less are not sufficient to form GP zones in alloys with zinc content lower than about 4% which could influence the η' formation, thus some other type of nucleation sites must exist at T_a.

Contrary to Al–Zn alloys, Al–Zn–Mg alloys are rather insensitive to the quenching conditions (quenching temperature T_q, and quenching rate, v_q) in the temperature range of natural ageing. Hardy [147], Polmear [31] and Gould [148] explained their results on the decomposition kinetics of Al–Zn–Mg alloys in dependence on T_q and T_a assuming that magnesium atoms are surrounded by clouds of zinc atoms and these complexes can trap vacancies. These complexes can be stable even at temperatures above the solubility limit. This is also supported by the correlated evaporation of zinc and magnesium atoms from Al–Zn–Mg alloy [98]. Hart [113] explained his experimental results by assuming that small groups of solute atoms and vacancies are diffusing. They can migrate like an "amoeba" and gradually agglomerate to form large clusters which are precipitate nuclei. The number, size and distribution of the clusters is assumed to be a function of the special heat treatment applied. The existence of clusters rich in vacancies has been supported recently also by positron lifetime and Doppler broadening measurements on Al–4.5%Zn–0.2 and 2.5%Mg alloys [149]. The results could be explained by assuming, that the positrons are trapped by complexes containing vacancies and solute atoms, and that the surrounding of the vacancies is rich mainly in zinc. These conclusions were later confirmed by other measurements [127].

Embury and Nicholson [11] investigated an Al–5.9 mass %Zn–2.9 mass %Mg alloy by means of TEM applying ageing between 80 and 180° C after DQ and IQ with two different cooling rates. The slower quenching rate (oil quench) resulted in a much coarser particle distribution after one hour ageing at 180° C compared to the samples quenched into water. They interpreted these results by the formation of VRC during rather short times (less than 30 sec) at room temperature the number of which depends sensitively on the quench procedure. These clusters are remarkably stable at 180° C (explained by the existence of a large binding energy between the vacancies and the groups of solute atoms) and can act as nucleation sites for metastable or stable phases.

According to Gjønnes and Simensen [7] after IQ to 130 and 150° C the η'-phase is present in an Al–Zn(5.77 mass %)–Mg(1.08 mass %) alloy, but not after a DQ treatment.

Holl [34] investigated an Al–5.48 mass %Zn–1.76 mass %Mg alloy by TEM and HV measurements applying different pre-ageing times at room temperature followed by an ageing at 80, 120 or 165° C ($T_h = 120°$ C in this alloy). The results of the long-time pre-ageing experiments were explained by the nucleation of η'-phase at over-critical size GP zones. The nuclei produced during quenching (and during very short pre-ageing times at room temperature) are different from the zones since an induction period is required after quenching before the room temperature pre-ageing exerts an effect on the development of HV during subsequent ageing. These additional nuclei most likely consist of some form of vacancy aggregates or vacancy–solute atom complexes. It is worth mentioning that the room temperature pre-ageing has no effect on the further ageing at 80° C.

Few years later Ryum [16, 57] interpreted the results of TEM and HV investigations made on an Al–2.48%Zn–1.24%Mg alloy also by the existence of some nuclei different from GP zones. This conclusion was based on the fact that a DQ to $T_a = 150° C > T_h$ yields no increase in hardness during ageing, but only 5 sec at room temperature after quenching is sufficient to result in good hardness values after proper ageing at 150° C, although the incubation time at room temperature for a remarkable increase in hardness amounts about 1000 sec. The existance of nuclei for η' particles formed at room temperature just after quenching was recently demonstrated by Kovács-Csetényi and Ryum [150] applying direct and interrupted (at 200° C) quench to room temperature and measuring the hardness of an Al–6 mass %Zn–1 mass %Mg alloy after ageing for 4 h at 150° C.

Zahra and co-workers [64, 139, 151] studied an Al–2.12%Zn–1.26%Mg alloy by means of TEM and microcalorimetric investigations. They found that above 115° C the dispersion of the η' particles depends on T_q (varied between 400 and 500° C), even after longer pre-ageing at $T_{pre} = 40°$ C. In

agreement with Ryum [16, 57] they concluded that VRC different from ZnV- and MgV-pairs, were quenched-in which are inactive but stable at low temperatures (near room temperature), and become active only at elevated temperatures as nucleation sites for the η' particles. These complexes are fairly stable and are not annealed out during short reversion treatments at 200° C, but they disappear during long term ageing near room temperature. The complexes are absent after interrupted quench, slow cooling to room temperature or quench to temperatures above 100° C [151]. It seems worth mentioning that Zahra *et al.* [64, 151] found evidence that the formation of η-phase is also influenced by these quenched-in nuclei.

De Ardo and Simensen [152] found no indication of nucleation sites for the η'-phase in an Al–6.8 mass %Zn–2.32 mass %Mg alloy after quenching from 465° C into oil at room temperature (holding time 10 sec) and subsequent ageing at elevated temperatures.

Kovács *et al.* [138] investigated an Al–2.0%Zn–1.4%Mg alloy by means of SAXS measurement of f, electrical resistivity, R, and yield stress, Y measurements applying different pre-ageing times at room temperature and a subsequent ageing of 2 h at 160° C ($> T_h$). The results obtained for these three quantities after the end of the 2 h ageing treatment at 160° C are shown in Fig. 5. It can be seen that a minimum occurs after about 30 min pre-ageing time at room temperature in each of the measured quantities. In order to clarify the reason of these minima TEM micrographs were taken after DQ to 160° C as well as IQ to 160° C

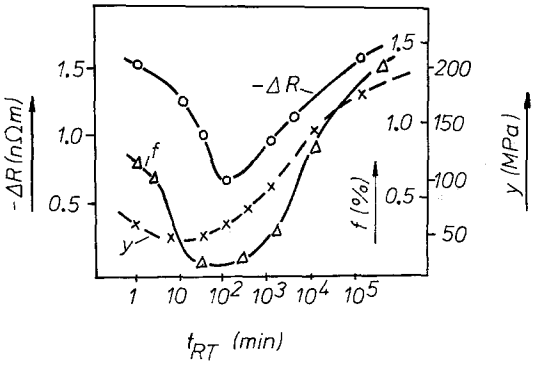

Figure 5 Yield stress, Y, volume fraction of η' precipitates, f, and change in electrical resistivity, ΔR, obtained at 160° C during two hours, as functions of pre-ageing time at room temperature.

[107]. In the latter case the pre-ageing time at room temperature was varied between 1 min and 6 h. Subsequently the samples were aged for 2 h at 160° C. The results obtained after room temperature ageing for 1 min, 30 min and 6 h are shown in Fig. 6. These results clearly indicate that minima of the parameters in Fig. 5, coincide with the absence of precipitates (gap of precipitation, see especially Fig. 6c). The absence of precipitates is also observed after DQ to 160° C (Fig. 6a). However, if the ageing time after IQ at room temperature is shorter (Fig. 6b) or longer (Fig. 6d) than 30 min, the formation of η'-phase at 160° C is possible.

Investigations done in a similar manner on an Al–4.5%Zn–2.5%Mg alloy (only the ageing was performed at 180° C $> T_h = 170°$ C) gave no sign on a gap of precipitation (see Fig. 7). However, in alloy Al–2.3%Zn–1.3%Mg a small indication of such a gap was observed [146].

These results can be explained on the basis that, both VRC and GP zones formed at room temperature can serve as nucleation sites for the η' particles. The VRC have an important effect in the nucleation of the η' particles only if the time of pre-ageing at room temperature is relatively short. As demonstrated in Fig. 6a, this type of nuclei do not form when the alloy is directly quenced to 160° C. The role of VRC in the formation of η' precipitates is relatively more significant in the case of lower concentration alloys, particularly at the beginning of the room temperature process.

According to Katz and Ryum [118] below the dissolution line of GP zones both the zones and VRC can act as nucleation sites for η', but above the dissolution line, up to the range of homogeneity, only VRC are effective.

It can be assumed that the number of VRC is decreasing with increasing pre-ageing time at room temperature most probably because they anneal out. The amount of zones providing nucleation sites for η' particles increases with increasing pre-ageing time and zinc content. The density of nucleation sites for the η' particles as a function of pre-ageing time at room temperature with the zinc content as a parameter is schematically shown in Fig. 8 [107, 138, 146].

The fact that a gap of precipitation exists in the low concentration Al–Zn–Mg alloys seems to be the most reliable proof that VRC really play an important role in the nucleation of the η'-phase.

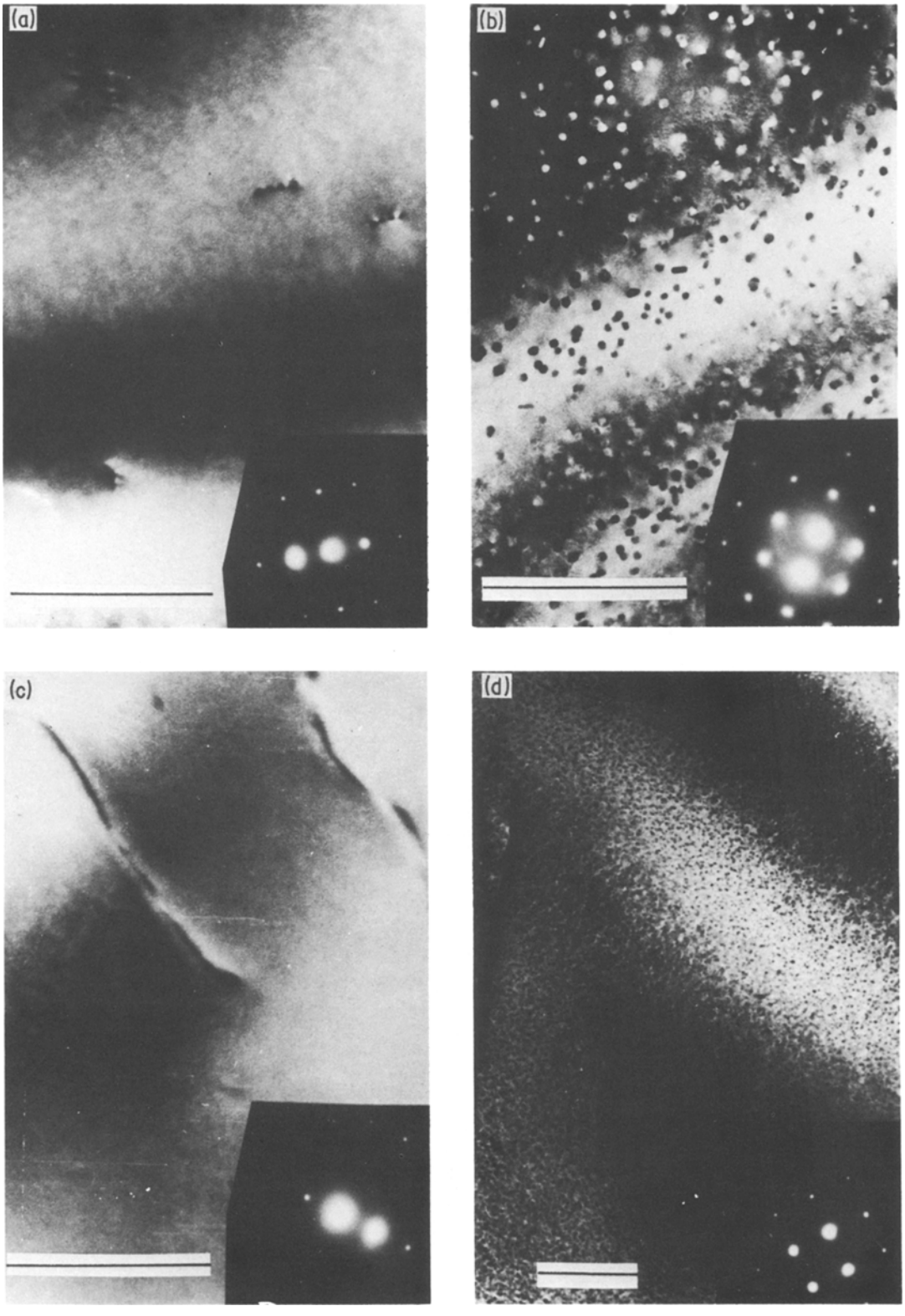

Figure 6 TEM micrographs of an Al–2%Zn–1.4%Mg alloy after 2 h ageing at 160° C following DQ to 160° C (a); quench to room temperature and 1 min (b), 30 min (c) and 6 h (d) pre-ageing at room temperature. (The marks indicate 250 nm.)

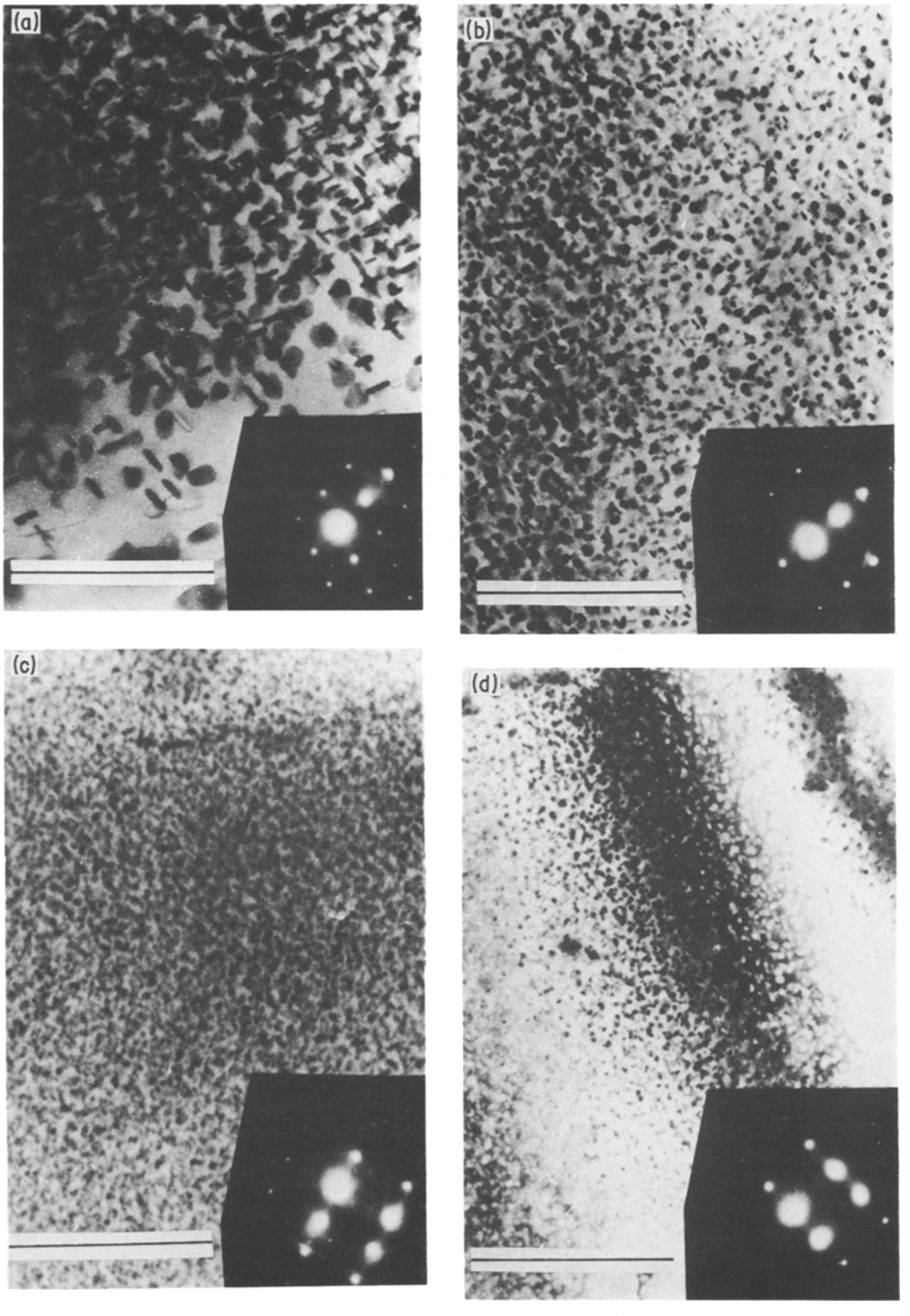

Figure 7 TEM micrographs of an Al–4.5%Zn–2.5%Mg alloy after 30 min ageing at 180° C following quench to room temperature and 15 min (a), 3 h (b), 12 h (c) and 3 days (d) pre-ageing at room temperature [107]. (The marks indicate 250 nm.)

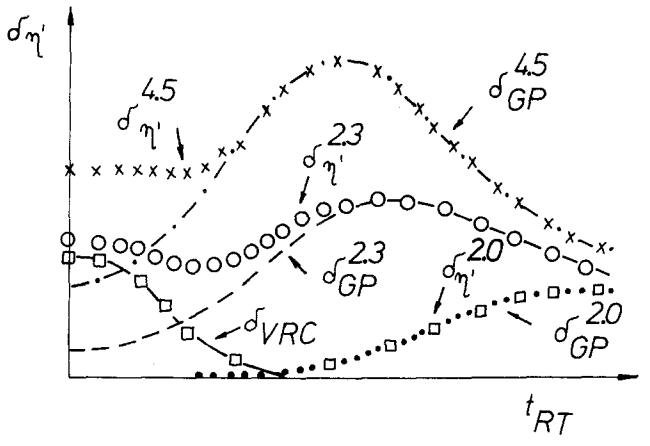

Figure 8 Schematic representation of the number of nucleation sites for the η' particles in dependence on pre-ageing time at room temperature for the case of 3 different Al–Zn–Mg alloys containing 4.5, 2.3, 2.0% Zn and 2.5, 1.3, 1.4% Mg, respectively. ($\delta^i_{\eta'}$: number of η' particles; δ^i_{GP}: number of GP zones suitable for η' nucleation; δ_{VRC}: number of VRC.)

3.4. The effect of impurity atoms on the nucleation

The technical Al–Zn–Mg alloys always contain additional elements. Some of them are purposely added in order to decrease the sensitivity of the alloy against stress corrosion, to obtain a fine grained material and so on. We do not deal with these problems, but only refer to the role of such minor elements in the nucleation processes of the metastable phases. We intend to summarize only some main features.

The impurity atoms may influence the decomposition processes for example in the following manner: they

(a) may form precipitates and sometimes consume alloying elements (for example Mg_2Si),

(b) can stabilize the GP zones (for example silver [153] and copper [44]),

(c) can decrease the formation energy of metastable precipitates (for example, lithium in AlCu) and

(d) can capture vacancies retarding in this manner the formation rate of GP zones (e.g. Si, V, Ti) [154].

Following Polmear [155] and Vietz *et al.* [156] Stefanovich [126] investigated the effect of silver on the ageing process of Al–Zn–Mg alloys. He investigated an Al–2.7%Zn–2.1%Mg alloy (produced from 5N material) with and without 0.05% additional silver. The addition of silver resulted in a good strength after ageing between 100 and 200° C, regardless of pre-ageing. This means that silver shifts up the temperature of the homogeneous nucleation of η' particles. An increase in the plasticity of the alloy was also observed.

Barczy and Gacsi [157, 158] examined the influence of silicon additions (0.002 and 0.10 mass %, respectively) on the decomposition behaviour of an Al–4.6 mass %Zn–1.5 mass %Mg alloy. Influence of silicon on the decomposition processes was found only between 100 and 225° C. The results show that simultaneous formation of Zn–Mg and Mg–Si particles takes place in this alloy. The existence of Mg–Si particles is shown by the facts that the reversion is only partial at 140° C, and the alloy containing 0.1 mass %Si shows a remarkable increase in hardness after DQ to 150° C.

The increment of hardness due to silicon additions after DQ was confirmed also by the investigation of an Al–4.52 mass %Zn–1.15 mass % Mg–0.43 mass %Si alloy (ageing at 160° C) [159]. An increase in the yield stress of an Al–3.2 mass % Zn–2.2 mass %Mg–0.25 mass %Si alloy at $T_a >$ 80° C was also explained by the additional formation of Mg_2Si-clusters [100]. However, from these measurements it cannot be uniquely concluded that the additional increment of hardness arises alone from the formation of Mg_2Si particles (because their amount seems to be too small related to the increase in the hardness), but a role of silicon or MgSi-clusters as nucleation sites of the η' particles is also possible.

The influence of titanium on the decomposition processes in Al–Zn–Mg alloys and the width of the precipitate free zones (PFZ) was investigated recently by Judd and his co-workers [160–163]. It was found that the coarsening of precipitate particles is remarkably retarded in titanium containing alloys. They explained this behaviour by assuming that titanium retards the kinetics of

precipitation in Al–Zn–Mg alloys by inhibition of solute diffusion in the matrix. It was also observed that in titanium containing alloys the width of the PFZ is considerably smaller (about three times) compared to the pure alloy [163]. From this result they concluded that titanium atoms narrow the vacancy depleted region near the grain boundaries relative to the ternary alloy which is probably a consequence of a strong interaction between vacancies and titanium atoms.

Bryant [164] studied the effect of copper, chromium and manganese upon the quench sensitivity of Al–Zn–Mg alloys (zinc content between 4.4 and 6.6 mass % and manganese content between 1.0 and 2.6 mass %). Little or no quench sensitivity was observed in the simple ternary alloys. The addition of copper, chromium or manganese makes the alloys with larger magnesium concentration (2.5 mass %Mg) quench sensitive, but the alloys with a lower magnesium concentration (1 mass %Mg) remain insensitive. It was concluded that at large magnesium concentrations these additional elements enhance the formation of incoherent phases during the quench.

Recently Gerlach and Löffler [165] investigated an Al–2.0%Zn–1.3%Mg alloy with and without technical impurities after DQ. The results show that in the alloy with additional elements clusters of the impurity atoms can act as nucleation sites for the heterogeneous formation of η' precipitates.

A maganese addition increases significantly the strength of the Al–Zn–Mg alloys. It is probable, however, that manganese does not influence the formation of ZnMg clusters but increases the strength independently from the ZnMg particles [166, 167].

According to Szentirmay and Groma [168] FeSi clusters play an important role in the nucleation of the η'-phase.

As a summary it can be concluded that clusters of impurity atoms can act as nucleation sites for the formation of metastable and stable phase particles.

3.5. Influence of the pre-ageing temperature on the stability of GP zones against reversion

In this section we summarize experimental results which show that the partial reversion is connected with the existence of GP zones able to transform directly into η' particles.

Only a little information is available about the stability of the zones against reversion as regards the dependence on the pre-ageing temperature. Asano and Hirano [18] investigated an Al–5.06 mass %Zn–0.94 mass %Mg alloy by means of DSC and HV measurements. They observed that both the rate and degree of reversion at 180° C depend considerably upon T_{pre}. After pre-ageing at room temperature the hardness decreased to the as-quenched value within 20 sec, while after 40° C pre-ageing it took 300 sec and complete reversion of the hardness did not take place on applying $T_{pre} = 70°$ C.

Prasad and Mallik [136] investigated Al–5.9 mass %Zn–1.43 mass % and 2.5 mass %Mg alloys by means of resistivity and HV measurements. After pre-ageing the samples at 60 and 100° C until the maximum of resistivity had been attained a reversion treatment was applied at 180° C (alloy containing 2.5 mass %Mg). After both pre-ageing treatments the reversion took place within 2 min at 180° C. The maximum hardness of samples after ageing at 180° C did not change for longer pre-ageing times than that belonging to the maximum of resistivity. This means that the further increase of the zone size did not result in an increase of the maximum hardness.

Lorimer and Nicholson [32] found also that the density of precipitate particles obtained during ageing at 180° C increased with pre-ageing time only up to 30 min at 100° C.

Korngiebel *et al.* [169] investigated the influence of pre-ageing temperature on the hardness of an Al–2.0%Zn–1.1%Mg alloy during ageing at 160° C. The result is shown in Fig. 9. It can be seen that in the alloy pre-aged at room temperature a larger amount of GP zones is dissolved than in the sample pre-aged at 70° C. Furthermore the specimen pre-aged at 70° C is less sensitive to overageing than the sample pre-aged at room temperature.

Kawano *et al.* [48] investigated the influence of the pre-ageing temperature on the reversion behaviour at 180° C of an Al–2.8%Zn–1.4%Mg alloy by means of SAXS and HV measurements. They found that pre-ageing both at room temperature and at 80° C, the ageing at 180° C results in finely distributed precipitates. The mean size of the precipitates attained after heat treatment at 180° C as a function of pre-ageing time is given in Table IV.

Although the size of the zones attained during pre-ageing treatments was not established in

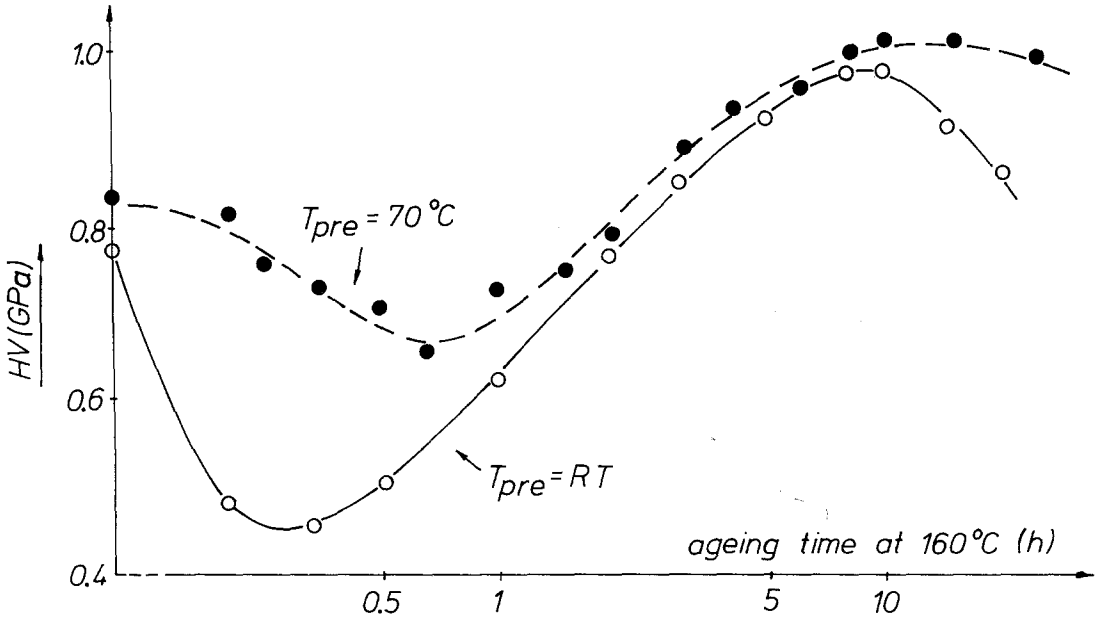

Figure 9 Changes in microhardness of an Al–2%Zn–1.1%Mg alloy during ageing at 160° C after 7 days pre-ageing at room temperature (open circles) or 32 h pre-ageing at 70° C (full circles) [169].

TABLE IV Mean radius of the precipitates, r_G, after ageing at 180° C up to hardness maximum [48]

Radius (nm)	Pre-ageing conditions Temperature/time
8.0	RT/10 min
6.2	RT/4 h
5.2	RT/7 days
5.4	80° C/5 min
4.4	80° C/48 h

general, one can conclude that the increasing stability of the zones against reversion with increasing T_{pre} is probably due to the increase in the mean size of the zones.

To study the effect of the mean particle size on the stability of zones an Al–4.5%Zn–2%Mg alloy was recently investigated [41] applying pre-ageing between room temperature and 100° C for ageing times to reach an average size in each case of 1.3 and 2.7 nm. For the reversion treatment the temperatures were selected between 160 and 200° C. As it can be seen from Fig. 10 during reversion treatment at 160° C three stages of the precipitation process can be distinguished. In stage 1 r_G remains approximately constant and Q_0 is decreasing. The same behaviour of r_G and Q_0 was observed by Gerstenberg [124] investigating the reversion of Al–2.5%Zn–1.0–2.9%Mg alloys. In this stage the main process is the dissolution of the unstable zones.

In stage 2 the size of precipitates starts to increase and Q_0 is also increasing up to about 85% of its maximum value. From these findings it can be concluded that in this stage the precipitates grow, at the expense of the zones dissolved in stage 1.

In stage 3 the growth rate of the precipitates becomes independent of the initial size of zones (Fig. 11) [41].

In Fig. 11 the change of r_G and Q_0 is shown as a function of ageing time at 180° C. The samples were pre-aged at 100° C to various sizes. From these results it can be concluded that the larger the size of the precipitates formed at a given pre-ageing temperature the smaller is the amount of the dissolved zones, resulting in their higher stability against reversion. In Fig. 12 r_G and Q_0 are shown as function of ageing time at T_r = 160, 180 and 200° C for samples with initial Guinier radii of particles $r_G = 1.3 \pm 2$ nm (Fig. 12a) and $r_G = 2.7 \pm 0.3$ nm (Fig. 12b) formed during pre-ageing at 100° C. It can be seen from this figure that starting with $r = 2.7$ nm and applying T_r = 160° C no decrease in integral intensity appears but starting with $r_G = 1.2$ nm and/or applying a higher T_r, Q_0 first decreases. This means that the stability of the particles formed during pre-ageing increases with increasing average size. The increase of the average particle size starts after a relatively long incubation period. This

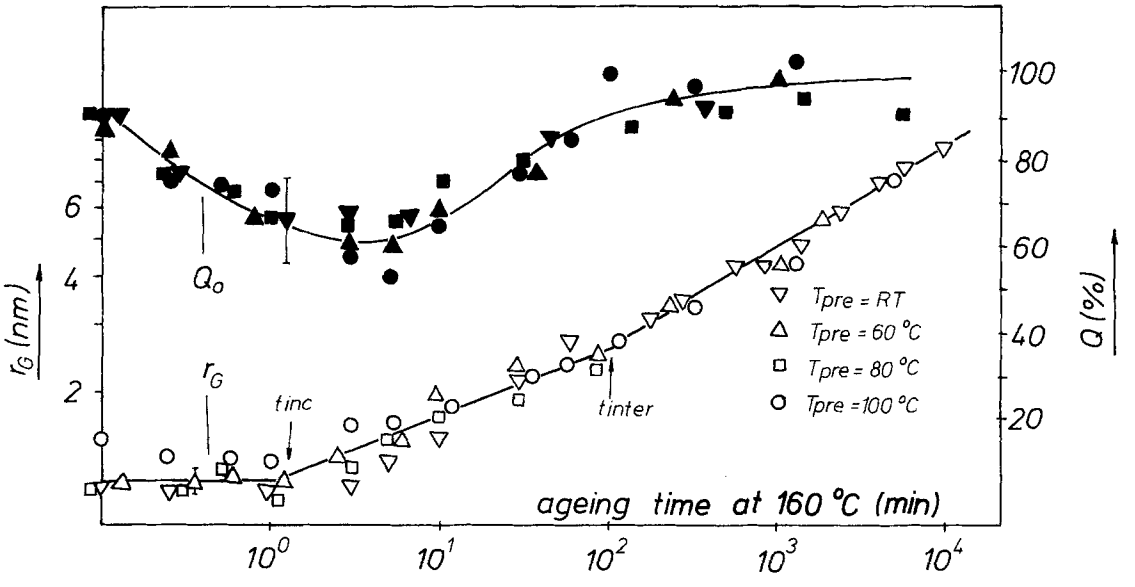

Figure 10 Changes in Guinier radius, r_G and in the integral intensity, Q_0, during 160° C reversion heat treatment of an Al–4.5%Zn–2%Mg alloy pre-aged at room temperature, 60, 80 and 100° C, respectively, to reach an average particle size of $r_G = 1.2 \pm 0.1$ nm [41].

means that precipitates grown at 100° C probably need some change in their internal structure before they start to coarsen by the Ostwald ripening process.

From these observations it is very probable that a critical size of precipitates exists at each T_r above which the particles are stable against dissolution. The critical size increases with increasing T_r. For $T_r = 160°$ C this critical value in the alloy investigated is between 2.0 and 2.7 nm and at $T_r = 180°$ C it is higher than 2.7 nm.

3.6. Reversed two-step ageing

The reversed two-step ageing is an ageing sequence in which the second ageing step is made at a lower temperature than the first one. Embury and Nicholson [11] investigated an Al–5.9 mass%Zn–2.9 mass%Mg alloy quenched directly to 180° C

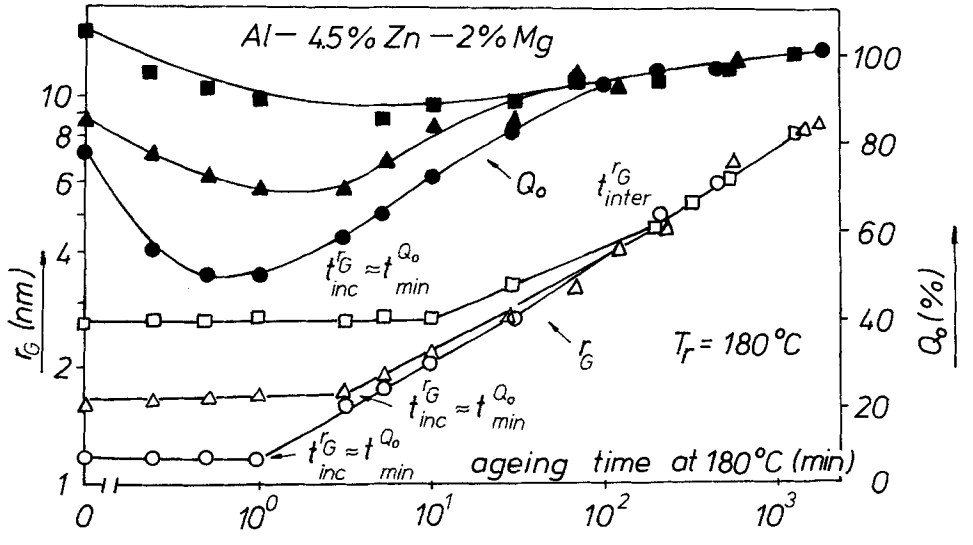

Figure 11 Changes of r_G and Q_0 during 180° C reversion heat treatment of samples pre-aged at 100° C to reach different average initial radii of the zones.

for 3 h and subsequently aged at 135° C. After the final ageing they observed two types of precipitates, namely lath shaped η' formed on dislocations at 180° C, and fine precipitation of the η'-phase formed at 135° C. They interpreted this observation by the existence of VRC which survive the treatment of 3 h at 180° C. The stability of these nuclei is explained by the strong binding between vacancies and groups of solute atoms.

The stability of some nuclei is also confirmed by cooling experiments (cooling rate 3 K min^{-1}) performed with two Al–4.5%Zn–2 ~ 3%Mg alloys [170]. It was observed that after passing T_h a dense system of GP zones was formed indicated by the steep increase of both SAXS intensities and extra-resistivity (see Fig. 13).

The microhardness of an Al–2.0%Zn–1.3%Mg alloy with technical impurities was investigated after direct quench as a function of ageing time at

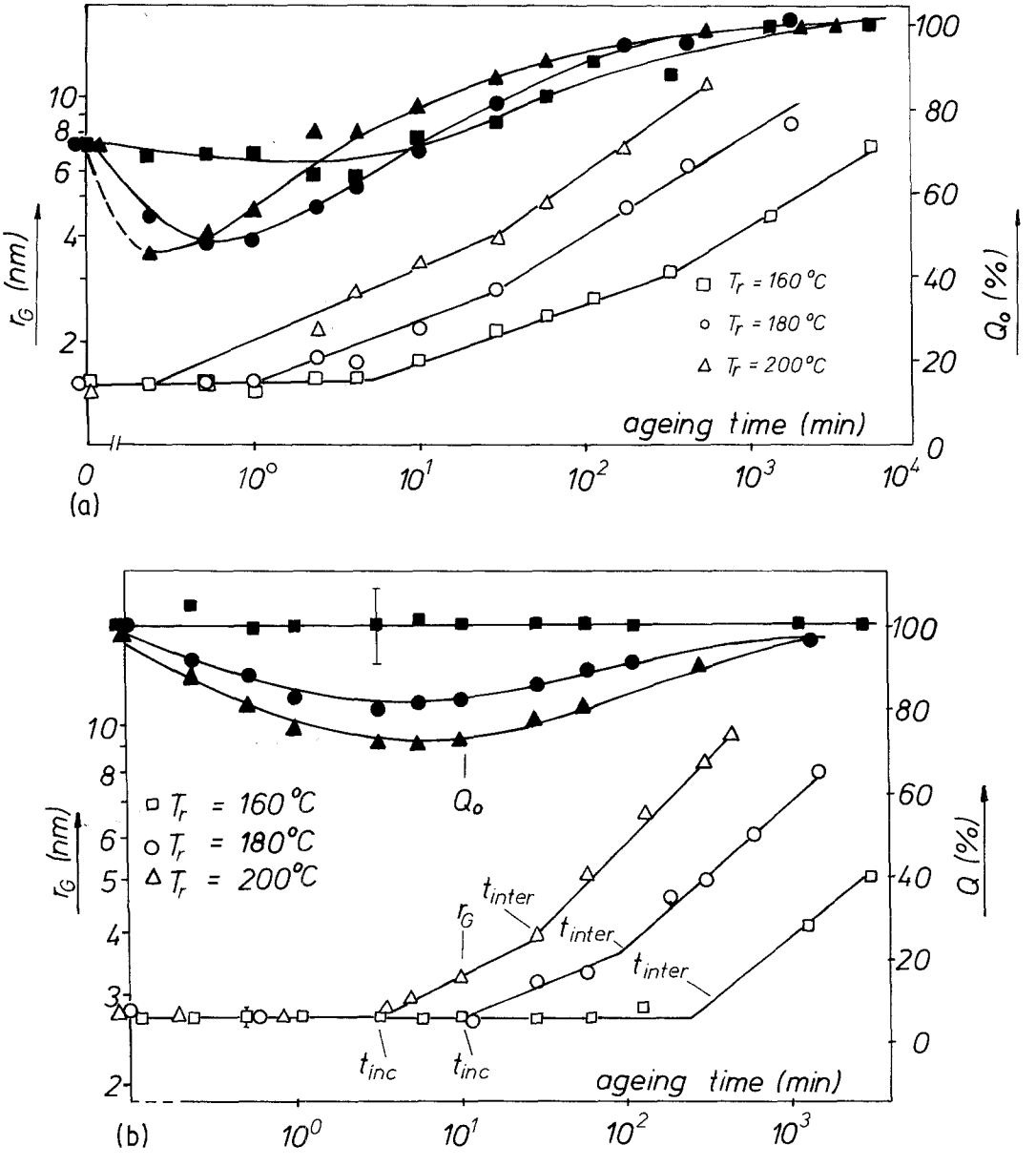

Figure 12 r_G and Q_0 against ageing time at T_r = 160, 180 and 200° C for samples with initial Guinier radii of particles r_G = 1.3 ± 0.2 nm (a) and r_G = 2.7 ± 0.3 nm (b), T_{pre} = 100° C.

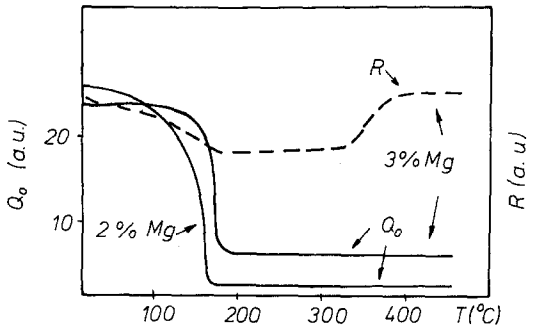

Figure 13 Changes in SAXS intensities, Q_0, and in extra resistivity, R, during 3 K min^{-1} cooling of Al–4.5%Zn–2 ~ 3%Mg alloys [170].

$T_a = 70$, 100, 110 and 160° C with and without further ageing at room temperature for 42 days [171]. The results are shown in Fig. 14. It can be seen that the hardness attained during room temperature ageing, does not depend on the previous ageing time if it is less than the incubation period. This means that no such structure changes take place during pre-ageing which could influence the room temperature ageing. Samples pre-aged up to $T_a = 90°$ C show normal behaviour after 42 days ageing at room temperature, but the specimens aged at $T_a = 100°$ C for periods somewhat longer than the incubation time show a distinct minimum after 42 days room temperature ageing . This is probably a consequence of the formation of η'-phase or of spherical hexagonal zones [58, 106] during pre-ageing decreasing therefore the amount of GP zones formed at room temperature.

3.7. Precipitate free zones

Precipitate-free zones (PFZ) are often observed in the vicinity of grain boundaries in age hardenable alloys. Due to their effect on the stress corrosion and mechanical properties of Al–Zn–Mg alloys the formation of PFZ was studied by many authors. The most important literature is listed in [172]. The formation of PFZ was originally attributed to the depletion of solute atoms caused by preferential precipitation at the grain boundaries [32, 78, 173–176]. However, it was pointed out that the local depletion of vacancies in the neighbourhood of grain boundaries might also be important in the formation of PFZ [11, 21, 32,

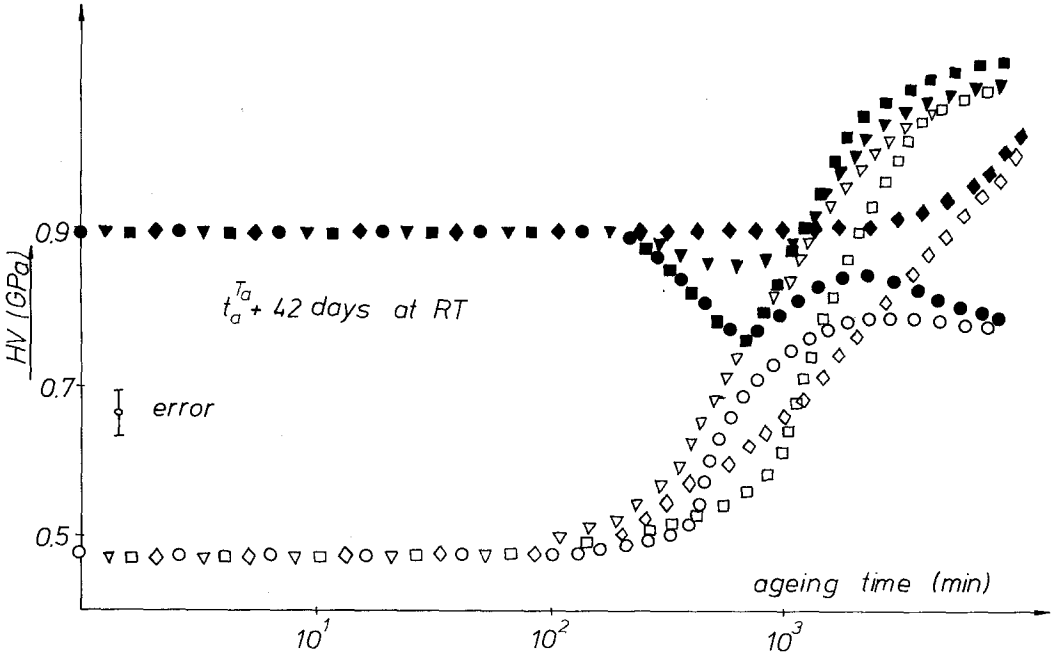

Figure 14 Changes in microhardness of an Al–2% Zn–1.3% Mg alloy of technical purity in dependence on the ageing time at 70° C (◇), 100° C ( ), 110° C (□) and 160° C (○) without (open symbols) and with 42 days postageing at room temperature (full symbols) [171].

78, 177–179]. According to Taylor [114] and Embury and Nicholson [11] the vacancies are important because a critical concentration is required for precipitate nucleation. The importance of both solute and vacancy concentration profiles in PFZ formation was emphasized in terms of the thermodynamics of precipitate nucleation and GP zone formation [28, 32, 178, 180]. An alternative explanation taking into account both vacancy and solute profiles in determining the width of PFZ was advanced by Pashley and co-workers [29. 110] considering the kinetics of precipitation.

More recently the solute concentration profiles could be directly determined by monitoring the plasmon loss of the electron beam in a TEM [181–184] by Auger electron spectroscopy (AES) [185] and by X-ray microanalysis [172, 186]. In the as-quenched samples an appreciable segregation of both zinc and magnesium atoms to the grain boundaries was observed. The AES plasmon loss results show [185] that in case of over-aged samples the zinc atoms in the PFZ are practically all in the form of $MgZn_2$ precipitates, while only about 40% of total magnesium is in the precipitates, the other 60% of magnesium being localized to within a few atomic layers of the grain boundary. The analysis of solute profiles in Al–Zn–Mg alloys indicate no significant solute depletion prior to ageing in the regions where PFZ are to be formed. This observation shows that the initiation of PFZ is primarily due to the vacancy concentration and the absence of precipitation is mainly due to the difficulties of nucleating precipitate particles directly from the supersaturated matrix [172]. Because of the absence of precipitation in the PFZ the solute concentration of the matrix in the PFZ remains for relatively long ageing times higher than that in the grain interior. On the other hand due to the grain boundary segregation and to the relatively easy heterogeneous nucleation of grain boundary precipitates the solute concentration becomes low in the immediate vicinity of grain boundaries. As a consequence of this a maximum appears in the matrix solute concentration profile near the border of the PFZ [18, 172, 185, 186]. The concentration gradients result in a diffusion flux towards the grain interior as well as towards the grain boundaries. Consequently the precipitates at the PFZ boundaries and in the grain boundaries attain larger average dimensions than the particles in the grain interior.

4. Conclusions

In this review an attempt has been made to discuss briefly some of the more important aspects of the characteristics of the decomposition processes in Al–Zn–Mg alloys. As a summary of the results discussed the following conclusions can be drawn.

After quenching to ageing temperatures, $T_a < T_h$ the decomposition of the supersaturated solid solution starts with the nucleation and growth of GP zones. The upper temperature limit of GP zone formation, T_h depends on the alloy composition and is between about 100 and 180° C.

Disregarding the very early stage of the decomposition the kinetics of GP zone formation is independent of the quenching conditions. It can be supposed that the growth of the zones is governed by the movement of MgV pairs.

Up to about 60° C only GP zone formation can take place. Between about 60° C and T_h the formation of both GP zones and η'-phase particles takes place. There are indications that in the latter temperature range two types of GP zones can exist in alloys low in magnesium ($< 0.5\%$) or in zinc ($< 3\%$) content. In alloys richer in magnesium and zinc only one type of GP zone seems to exist. Near T_h spherical hexagonal zones can also be observed.

The nucleation of the η'-phase most probably can take place only at preferred nucleation sites. Such nucleation sites can be the following:

(a) concentration fluctuation left behind by dissolving GP zones in low concentration ($C_{Zn} \lesssim 2.5\%$) alloys

(b) GP zones of overcritical size

(c) quenched-in clusters rich in vacancies

(d) impurity atom clusters.

The dispersion of the η' particles formed during ageing at temperatures, $T > T_h$ depends sensitively on the quench conditions (amount of VRC) as well as on the pre-ageing treatment (size distribution of the GP zones).

A dense system of finely distributed η' particles which yields good strength and narrow precipitate free zone can be obtained by pre-ageing the samples at $T < T_h$ for times sufficient to reach a suitable size of GP zones and applying a final ageing at temperatures $T > T_h$ ($T \approx T_h + 30\,K$).

Impurity atoms can assist the nucleation of the η'-phase but it has to be taken into account that in such cases intermetallic phases can also be formed which may trap zinc and magnesium atoms.

The stability of the GP zones against reversion heat treatments increases with increasing zone sizes.

Finally it can be stated that although a very significant progress has been made over the last ten years in the understanding of the nature of decomposition of Al–Zn–Mg alloys, it is clear that many questions remain unanswered both for theoretical and experimental points of view.

References

1. W. KÖSTER and W. WOLF, *Z. Metallkd.* **28** (1936) 155.
2. W. KÖSTER and W. DULLENKOPF, *ibid.* **28** (1936) 309, 363.
3. L. F. MONDOLFO, *Int. Metall. Rev.* **153** (1971) 95.
4. W. B. PEARSON, "Handbook of Lattice Spacing and Structure of Metals and Alloys" (Pergamon Press, Oxford, 1958).
5. L. F. MONDOLFO, "Aluminium Alloys: Structure and Properties" (Butterworths, London, 1976).
6. H. P. DEGISCHER, W. LACOM, A. ZAHRA and C. ZAHRA, *Z. Metallkd.* **71** (1980) 231.
7. J. GJØNNES and C. J. SIMENSEN, *Acta Met.* **18** (1970) 881.
8. H. SCHMALZRIED and V. GEROLD, *Z. Metallkd.* **49** (1958) 291.
9. P. A. THACKERY, *J. Inst. Met.* **96** (1968) 228.
10. P. AUGER, J. M. RAYNAL, M. BERNOLE and R. GRAF, *Mem. Sci. Rev. Met.* **9** (1974) 557.
11. J. D. EMBURY and R. B. NICHOLSON, *Acta Metall.* **13** (1965) 403.
12. L. F. MONDOLFO, "Metallography of Aluminium Alloys" (J. Wiley, New York 1943).
13. K. RIEDERER, *Z. Metallkd.* **28** (1936) 312.
14. G. BERGMANN, J. L. T. WAUGH and L. PAULING, *Acta Cryst.* **10** (1957) 254
15. I. N. FRIDLYANDER, N. S. GERCHIKOVA and N. I. ZAITSEVA, *Metalloved. Term. Obrab. Met.* **1966 (8)** (1966) 11.
16. N. RYUM, *Z. Metallkd.* **66** (1975) 377.
17. E. H. DIX, *Trans. ASM* **42** (1950) 1057.
18. K. ASANO and K. HIRANO, *Trans. JIM* **9** (1968) 24.
19. A. KELLY and R. B. NICHOLSON, *Progr. Mater. Sci.* **10** (1963) 1.
20. L. F. MONDOLFO, N. A. GJOSTEIN and D. W. LEWINSON, *TAIMME* **206** (1956) 1378.
21. G. THOMAS and J. NUTTING, *J. Inst. Met.* **88** (1959–60) 81.
22. R. B. NICHOLSON, G. THOMAS and J. NUTTING, *ibid.* **87** (1958–59) 429.
23. R. B. NICHOLSON, G. THOMAS and J. NUTTING, *Brit. J. Appl. Phys.* **9** (1958) 25.
24. V. M. PASALSKI and A. F. POLESIA, *Fiz. Metall. Metallov.* **23** (1967) 60.
25. V. B. SPIRIDONOV, T. A. VLASOVA and V. N. JORDANSKI, *Metalloved. Term. Obrab. Met.* **1966/8** (1966) 607.
26. T. WILLIAMS, *J. Inst. Met.* **91**, (1962–63) 324.
27. L. F. MONDOLFO, *ibid.* **97** (1969) 95.
28. G. W. LORIMER and R. B. NICHOLSON, "The Mechanism of Phase Transformations in Crystalline Solids" (Institute of Metals, London, 1969) p. 36.
29. M. H. JACOBS and D. W. PASHLEY, *ibid.* p. 43.
30. I. J. POLMEAR, *J. Inst. Met.* **87** (1958–59) 24.
31. *Idem, ibid.* **86** (1957) 113.
32. G. W. LORIMER and R. B. NICHOLSON, *Acta Metall.* **14** (1966) 1009.
33. Y. MURAKAMI, O. KAWANO and H. TAMURA, *Mem. Fac. Eng. Kyoto Univ.* **25** (1963) 303.
34. H. A. HOLL, *Met. Sci. J.* **1** (1967) 111.
35. R. GRAF, *J. Inst. Met.* **86** (1957–58) 534.
36. B. GENTRY, R. GRAF and G. LENIOR, *Compt. Rend.* **247** (1958) 1731, 2126.
37. G. THOMAS, *J. Inst. Mat.* **86** (1957–58) 536.
38. A. V. DOBROMISLOV, O. D. SASOV and N. N. BUINOV, *Fiz. Met. Metalloved.* **24** (1967) 192.
39. S. E. NAESS, *Scripta Metall.* **3** (1969) 179.
40. K. HIRANO and Y. TAKAGI, *J. Phys. Soc. Jpn.* **10** (1955) 187.
41. B. GUEFFROY and H. LÖFFLER, *Phys. Status Solidi (a)* **66** (1981) 585.
42. N. RYUM, *Acta Metall.* **16** (1968) 327.
43. H. G. FABIAN and H. LÖFFLER, *Phys. Status Solidii (a)* **36** (1976) 127.
44. R. W. GOULD and E. A. STARKE, *Advan. X-Ray Anal.* **9** (1966) 59.
45. N. RYUM, *Acta Metall.* **17** (1969) 269.
46. P. BARDHAN and E. A. STARKE, *J. Mater. Sci.* **3** (1968) 577.
47. H. A. HOLL, *J. Inst. Met.* **97** (1969) 200.
48. V. O. KAWANO, Y. MURAKAMI, T. NAKAZAWA and K. S. LIU, *Trans, Jpn. Inst. Met.* **11** (1970) 12.
49. P. A. THACKERY and A. T. THOMAS, *J. Inst. Met.* **99** (1971) 114.
50. K. HIRANO and K. ASANO, *Trans. Jpn. Inst. Met.* **11** (1970) 225.
51. H. SUZUKI, M. KANNO and S. ASAMI, *Keikinzoku* **22** (1972) 269.
52. H. SUZUKI, S. ASAMI and M. KANNO, *ibid.* **22** (1972) 52.
53. S. CERESARA and P. FIORINI, *Meter. Sci. Eng.* **10** (1972) 205.
54. K. HIRANO, "Thermal Analysis: Comparative Studies on Materials", edited by H. Kambe and P. D. Garn (John Wiley and Sons, New York, 1974) p. 42.
55. K. H. DÜNKELOH, G. KRALIK and V. GEROLD, *Z. Metallkd.* **65** (1974) 291.
56. Y. TOMITA, K. S. LIU, Y. MURAKAMI and M. MORINAGA, *Trans. Jpn. Inst. Met.* **15** (1974) 99.
57. N. RYUM, *Z. Metallkd.* **66** (1975) 338, 344.
58. C. E. LYMAN and J. B. VANDER SANDE, *Met. Trans.* **74** (1976) 1211.
59. P. E. MARTH, H. I. AARONSON, G. W. LORIMER, T. L. BARTEL and K. C. RUSSELL, *Met. Trans.* **74** (1976) 1519.
60. K. ASANO, M. ABE and A. FUJIWARA, *Mater. Sci. Eng.* **22** (1976) 61.
61. P. J. BROFMAN and G. JUDD, *Met. Trans.* **94** (1978) 457.
62. E. HORNBOGEN, *ibid.* **94** (1978) 134.
63. A. MELANDER and P. A. PERSSON, *Acta Metall.*

26 (1978) 267.
64. A. ZAHRA, C. Y. ZAHRA, M. LAFFITTE, W. LACOM and H. P. DEGISCHER, *Z. Metallkd.* **70** (1979) 172.
65. R. GRAF, *Compt. Rend.* **242** (1956) 1311.
66. *Idem, ibid.* **244** (1957) 337.
67. V. GEROLD and W. SCHWEIZER, *Z. Metallkd.* **52** (1961) 76.
68. R. BAUR and V. GEROLD, *Acta Metall.* **10** (1962) 637.
69. V. GEROLD, Proceedings of the Conference on Small Angle X-ray Scattering, edited by H. Brumberger (Gordon and Breach, New York, 1966) p. 277.
70. K. H. DÜNKELOH, V. GEROLD and G. KRALIK, Proceedings of the 3rd International Conference on Strength Metals and Alloys, Cambridge, August 1973, Vol. 1, p. 296.
71. V. GEROLD, *J. Appl. Cryst.* **10** (1977) 25.
72. V. GEROLD, J. E. EPPERSON and G. KOSTORZ, *ibid.* **10** (1977) 28.
73. G. GROMA, I. KOVÁCS, E. KOVÁCS-CSETÉNYI, J. LENDVAI and T. UNGÁR, *Phil. Mag. A.* **40** (1979) 653.
74. V. GEROLD, *Phys. Status. Solidi* **1** (1961) 37.
75. H. SUZUKI, M. KANNO and K. FUKUNAGA, *J. Jpn. Inst. Light Met.* **22** (1972) 286.
76. G. HONYEK, I. KOVÁCS, J. LENDVAI, NG-HUY-SINH, T. UNGÁR, H. LÖFFLER and R. GERLACH, *J. Mater. Sci.* **16** (1981) 270.
77. M. RADOMSKY and H. LÖFFLER, *Krist. u.Techn.* **15** (1980) 703.
78. A. J. CORNISH and M. K. B. DAY, J. Inst. Met. 97 (1969) 44.
79. H. INOUE, T. SATO, Y. KOJIMA and T. TAKAHASHI, *Metall. Trans. A.* **12A** (1981) 1429.
80. T. UNGÁR, J. LENDVAI and I. KOVÁCS, *Aluminium* **55** (1979) 663.
81. R. GRAF, *Compt. Rend.* **243** (1956) 2834.
82. V. GEROLD and V. HABERKORN, *Z. Metallkd.* **50** (1959) 568.
83. T. UNGÁR, *ibid.* **70** (1979) 739.
84. J. LENDVAI, G. HONYEK and I. KOVÁCS, *Scripta Metall.* **13** (1979) 593.
85. C. PANSERI and T. FEDERIGHI, *Acta Metall.* **11** (1963) 575.
86. G. BARTSCH, *ibid.* **12** (1964) 270.
87. M. MURAKAMI, O. KAWANA and Y. MURAKAMI, *ibid.* **17** (1969) 29.
88. V. GEROLD, W. MERZ and O. KAWANO, *Z. Metallkd.* **61** (1970) 102.
89. H. BOSSAC, H. G. FABIAN and H. LÖFFLER, *Phys. Status Solidi (a)* **48** (1978) 369.
90. H. BOSSAC and H. LÖFFLER, *Neue Hütte* **24** (1979) 264.
91. H. G. FABIAN, P. TAPLICK and H. HÖFFLER, *Phys. Status Solidi (a)* **13** (1972) K169.
92. G. JÜRGENS, M. KEMPE and H. LÖFFLER, *ibid.* **21** (1974) K39.
93. H. SUZUKI, M. KANNO and S. ASAMI, *J. Jpn. Inst. Light Met.* **22** (1972) 269.
94. G. JÜRGENS, M. KEMPE and H. LÖFFLER, *Phys. Status Solidi (a)* **25** (1974) K73.
95. G. JÜRGENS and M. KEMPE, *Neue Hütte* **21** (1976) 166.
96. N. RYUM, *Acta Metall.* **17** (1969) 821.
97. G. GROMA and Z. SZENTIRMAY, *Scripta Metall.* **12** (1978) 991.
98. E. HIDVÉGI and E. KOVÁCS-CSETÉNYI, "Thermal Analysis", edited by H. Chihora (Kagaky Gijutu-Sha, Japan, 1977). p. 204.
99. A. JUHÁSZ, P. TASNÁDI, I. KOVÁCS and T. UNGÁR, *J. Mater, Sci.* **16** (1981) 367.
100. T. UNGÁR, J. LENDVAI, I. KOVÁCS, G. GROMA and E. KOVÁCS-CSETÉNYI, *ibid.* **14** (1979) 671.
101. E. KOVÁCS-CSETÉNYI, G. GROMA, J. LENDVAI, T. UNGÁR and I. KOVÁCS, *Aluminium* **57** (1981) 472.
102. W. KÖSTER and K. KAM, *Z. Metallkd.* **30** (1935) 320.
103. J. HERENGUEL and G. CHAUDRON, *Metaux Corros.* **16** (1941) 33, 49.
104. J. H. AULD and S. Mck. COUSLAND, *Scripta Metall.* **5** (1971) 765.
105. *Idem, J. Aust. Inst. Met.* **19** (1974) 194.
106. A. C. CHOU, *Scripta Metall.* **12** (1978) 421.
107. M. RADOMSKY, H. LÖFFLER, J. LENDVAI, T. UNGÁR and I. KOVÁCS, *Krist. Techn.* **15** (1980) 721.
108. P. E. ROPER and J. D. MARTIN, *Z. Metallkd.* **70** (1979) 400.
109. B. BOZIC, A. MIHAJLOVIC and D. MIHAJLOVIC, *Bull. T. LXV Acad. Serbe Sci. Arts Sci. Techn.* **15** (1979) 1.
110. D. W. PASHLEY, M. H. JACOBS and J. T. VIETZ, *Phil. Mag.* **16** (1967) 51.
111. D. W. PASHLEY, J. RODES and A. SENDOREK, *J. Inst. Met.* **94** (1966) 41.
112. R. R. ROMANOVA, *Fiz. Met. Metall.* **23** (1967) 89.
113. E. W. HART, *Acta Metall.* **6** (1958) 553.
114. J. L. TAYLOR, *J. Inst. Met.* **92** (1963–64) 301.
115. J. D. EMBURY and R. B. NICHOLSON, *ibid.* **93** (1964–65) 364.
116. K. C. RUSSELL, *Scripta Metall.* **3** (1969) 313.
117. M. R. MRUZIK and K. C. RUSSELL, *J. Nucl. Mater.* **78** (1978) 343.
118. Z. KATZ and N. RYUM, *Scripta Metall.* **15** (1981) 265.
119. M. L. V. GAYLER, *J. Inst. Met.* **28** (1922) 213.
120. W. FRAENKEL and L. MARX, *Z. Metallkd.* **21** (1929) 2.
121. K. L. MEISSNER, *J. Inst. Met.* **41** (1929) 234.
122. G. D. PRESTON and M. L. V. GAYLER, *ibid.* **41** (1929) 191.
123. V. GEROLD, *Z. Metallkd.* **45** (1954) 593.
124. K. W. GERSTENBERG, Dissertation A, Universität Stuttgart (1980).
125. H. BOSSAC, H.-G. FABIAN, O. KABISCH and H. LÖFFLER, *Neue Hütte* **21** (1976) 560.
126. V. M. STEFANOVICH, *Scripta Metall.* **14** (1980) 389.
127. O. KABISCH, G. DLUBEK, H. LÖFFLER, O. BRÜMMER and R. GERLACH, *Phys. Status Solidi (a)* **59** (1980) 731.
128. R. KROGGEL, H. LÖFFLER, E. KORNGEIBEL and G. ZOCH, *Krist. Techn.* **12** (1977) 1045.

129. K. -H. SACKEWITZ, M. RADOMSKY, H. LÖFFLER, O. KABISCH, T. UNGÁR, G. HONYEK, J. LENDVAI and I. KOVÁCS, *Krist. Techn.* **14** (1979) 457.
130. M. RADOMSKY, O. KABISCH, H. LÖFFLER, J. LENDVAI, T. UNGÁR, I. KOVÁCS and G. HONYEK, *J. Mater, Sci.* **14** (1979) 2906.
131. R. De IASI and P. N. ADLER, *Met. Trans.* **8A** (1977) 1177.
132. I. KOVÁCS, J. LENDVAI, T. UNGÁR, *Wiss. Zeitung PH Halle,* **15** (1977) 34.
133. H. -G. FABIAN, M. RADOMSKY, H. LÖFFLER and B. GUEFFROY, *Freiberger Forschungsh.* **B217** (1980) 97.
134. H. LÖFFLER, M. RADOMSKY, E. KORNGEIBEL, B. GUEFFROY and R. GERLACH, Proceedings of Kozubnik, Poland, September1980 (Silesian University, Katowice, 1980) p. 201.
135. G. HONYEK, I. KOVÁCS, J. LENDVAI, NG-HUY-SINH, T. UNGÁR, H. LÖFFLER and R. GERLACH, *Magyar Aluminium* **18** (1981) 39.
136. B. PRASAD and A. K. MALLIK, *Metallography* **6** (1973) 527.
137. J. T. HESLEY and R. W. GOULD, *Metall. Trans.* **8A** (1977) 1907.
138. I. KOVÁCS, J. LENDVAI, T. UNGÁR, K. BANIZS and J. LAKNER, *Aluminium* **53** (1977) 497.
139. W. LACOM, H. P. DEGISCHER and A. ZAHRA, Proceedings of the 7th Interanational Light Metal Congress, Leoben/Vienna, June 1981 (Aluminium Verlag, Düsseldorf, 1981) p. 182.
140. K. HIRANO, R. G. AGARWAL and M. COHEN, *Acta Metall.* **10** (1962) 857.
141. J. LENDVAI, I. KOVÁCS, Y. UNGÁR, J. LAKNER and K. BANIZS, *Aluminium* **56** (1980) 453.
142. C. G. CORDOVILLA and E. LOUIS, Proceedings of the 7th Interantional Light Metal Congress, Leoben/Vienna, 1981, p. 184.
143. G. GROMA and E. KOVÁCS-CSETÉNYI, *Phil. Mag.* **32** (1975) 869.
144. G. GROMA, E. KOVÁCS-CSETÉNYI, I. KOVÁCS, J. LENDVAI and T. UNGÁR, *Z. Metallkd.* **67** (1976) 404.
145. T. UNGÁR, J. LENDVAI, I. KOVÁCS, G. GROMA and E. KOVÁCS-CSETÉNYI, *Z. Metallkd.* **67** (1976) 683.
146. H. LÖFFLER, E. KORNGIEBEL and R. GERLACH, *Cryst. Res. Techn.* **16** (1981) 475.
147. H. K. HARDY, *J. Inst. Met.* **79** (1951) 321.
148. R. W. GOULD, *Advan. X-ray Anal.* **10** (1967) 185.
149. G. DLUBEK, O. BRÜMMER, J. YLI-KAUPPILS and P. HAUTOJÄRVI, Helsinki University of Technology; Report TKK-FA 416.
150. E. KOVÁCS-CSETÉNYI and N. RYUM, *Scripta Metall.* **15** (1981) 705.
151. A. ZAHRA, C. Y. ZAHRA, W. LACOM and H. P. DEGISCHER, *Mém. Sci. Rev. Mét.* **78** (1981) 17.
152. A. J. De ARDO and C. J. SIMENSEN, *Met Trans.* **4** (1973) 2413.
153. F. J. KIEVITZ and A. J. ZUITHEFF, *Aluminium* **46** (1970) 760.
154. Z. SZENTIRMAY and G. GROMA, *Aluminium* **57** (1981) 534.
155. I. J. POLMEAR, *J. Inst. Met.* **89** (1960–61) 193.
156. J. T. VIETZ, K. R. SARGANT and I. J. POLMEAR, *ibid.* **92** (1963–64) 327.
157. P. BARCZY and Z. GACSI, *Freiberger Forschungsh.* **B217** (1980) 75.
158. *Idem*, Proceedings of 2nd ICAAA, Visegrad, Hungary, April 1979 (Aluterv-fui, Budapest, 1979).
159. A. GOBLIRSCH, Diploma work, Pedagogical University, Halle (1981).
160. C. CHEN and G. JUDD, *Met. Trans.* **9A** (1978) 457.
161. C. A. GROVE and G. JUDD, *ibid.* **4A** (1973) 1023.
162. C. CHEN, PhD thesis, Rensselaer Polytechnic Institute, Trpy, New York (1976).
163. C. CHEN and G. JUDD, *Met. Trans.* **9A** (1978) 553.
164. A. J. BRYANT, *J. Inst. Met.* **94**, (1966) 94.
165. R. GERLACH and H. LÖFFLER, *Cryst. Res. Techn.* **17** (1982) 101.
166. H. WESTENGEN, O. REISO and L. AURAN, *Aluminium* **56** (1980) 768.
167. E. KORNGEIBEL, R. GERLACH and H. LÖFFLER, in preparation.
168. Z. SZENTIRMAY and G. GROMA, Proceedings of the 2nd ICAAA, Visegrad, Hungary, April 1979 (Aluterv-fui, Budapest, 1979) p. 13.
169. E. KORNGIEBEL, H. LÖFFLER and R. GERLACH, Research Report Pedagogical University Halle (1980) unpublished.
170. M. RADOMSKY, O. KABISCH, H. LÖFFLER, K. -H. SACKEWITZ, G. HONYEK, T. UNGÁR, J. LENDVAI and I. KOVÁCS, *Krist. Techn.* **14** (1979) 625.
171. R. GERLACH and H. LÖFFLER, *Cryst. Res. Techn.* **17** (1982) 267.
172. M. RAGHAVAN, *Met. Trans.* **11A** (1980) 993.
173. A. H. GEISLER, "Phase Transformations in Solids" (Wiley, New York, 1951).
174. H. S. ROSENBAUM and D. TURNBULL, *Acta Metall.* **6** (1958) 653.
175. H. S. ROSENBAUM, D. TURNBULL and E. J. ALESSANDRINI, *ibid.* **7** (1959) 678.
176. J. B. CLARK, *ibid.* **12** (1964) 1197.
177. H. S. ROSENBAUM and D. TURNBULL, *ibid.* **7** (1959) 664.
178. P. N. T. UNWIN, G. W. LORIMER and R. B. NICHOLSON, *ibid.* **17** (1969) 1363.
179. P. N. T. UNWIN and R. B. NICHOLSON, *ibid.* **17** (1969) 1379.
180. H. A. HOLL, *J. Inst. Met.* **93** (1964–65) 364.
181. P. DOIG, J. W. EDINGTON and G. HIBBERT, *Phil. Mag.* **28** (1973) 971.
182. P. DOIG and J. W. EDINGTON, *Brit. Corros. J. Quart.* **9** (1974) 220.
183. *Idem, ibid.* **9** (1974) 461.
184. *Idem, Met. Trans,* **6A** (1975) 943.
185. C. M. CHEN, T. S. SUN, M. K. VISWANASHAM and K. A. S. GREEN, *Met. Trans.* **8A** (1977) 1935.
186. M. RAGHAVAN, in 38th Annual Proceedings of the Electron Microscopy Society of America, San Francisco, California, 1980, edited by G. W. Bailey, p.94.

Received 15 November
and accepted 20 December 1982